Aus der Klinik für Augenheilkunde

der Medizinischen Fakultät Charité – Universitätsmedizin Berlin

DISSERTATION

Reliability of magnetic resonance imaging as a diagnostic tool for lacrimal gland tumors and predictors of a correct image-based diagnosis

zur Erlangung des akademischen Grades

Doctor medicinae (Dr. med.)

vorgelegt der Medizinischen Fakultät

Charité – Universitätsmedizin Berlin

von

Sérgio Filipe Alves Macedo

aus Lissabon

Datum der Promotion: 26.06.2022

Contents

List of Tables……....4

List of Figures……..…….6

List of Abbreviations……..……7

Zusammenfassung…….…….9

Abstract……..…….....11

1. Introduction…….……...…….....13

1.1. Anatomy, Development, and Physiology of the human lacrimal secretory system..….13

1.1.1 Anatomy of the human lacrimal secretory system…….....….13

1.1.2 Development of the human lacrimal secretory system……..17

1.1.3 Physiology of the human lacrimal secretory system.……18

1.1.3.1 The human tear film and its secretion……..…18

1.2 Clinicopathology of the human lacrimal gland……22

1.2.1 Benign primary epithelial tumors of the lacrimal gland……...24

1.2.2 Primary epithelial malignancies of the lacrimal gland……25

1.2.3 Non-Epithelial lesions of the lacrimal gland…….25

1.2.3.1 Dacryoadenitis…….25

1.2.3.2 Lymphoproliferative lesions of the lacrimal gland……...27

1.3 Imaging of the human lacrimal gland……29

1.4 Purpose of this thesis……....33

2. Materials and Methods……...35

2.1 Materials……..……35

2.1.1 Patients……..……..35

2.1.1.1 Inclusion criteria..……..……..35

2.1.1.2 Exclusion criteria…..……..……..37

2.2 Methods……..…….38

2.2.1 Clinical data……..……...…….38

2.2.2 Statistics……..……39

2.2.3 Ethics……..…….41

3 Results……..……...42

4 Discussion……...……....65

4.1 General cohort's clinical data and incidence of human lacrimal gland lesions…..…….65

4.2 Reliability of magnetic resonance imaging as a diagnostic tool for human lacrimal gland tumors in a clinical setting…….69

4.3 Analysis of our cohort's clinical data and search for predictors of a correct image-based diagnosis.....……..…..……..74

4.3.1 Signs and symptoms of human lacrimal gland tumors..……..…74

4.3.2 Features of the cohort's magnetic resonance imaging data……..76

4.4 Limitations of this study……..78

4.5 Other data points and final commentary……..……80

5 References……..81

6 Eidesstattliche Versicherung ……..……..92

7 Lebenslauf……93

8 Publikationsliste …..……...…95

9 Danksagung……96

List of Tables

Table	1	Lesions of the human lacrimal gland and their incidence	23
Table	2	Types of PEMLG and their incidence	24
Table	3	Etiology of dacryoadenitis	26
Table	4	Common ocular adnexal lymphomas and their incidence	28
Table	5	Standard imaging characteristics of lesions of the human lacrimal gland	31
Table	6	ICD-10 codes	35
Table	7	OPS codes	36
Table	8	Patient demographics	42
Table	9	Incidence rate of biopsied lacrimal gland tumors at the Charité Berlin between 2011 and 2018	43
Table	10	Patients' pre-operative clinical data	44
Table	11	Observed cases of lymphoma	45
Table	12	Crosstabulation of pre-operative orbital MRI diagnosis and corresponding histopathologic diagnosis	45
Table	13	Degree of correspondence between pre-operative orbital MRI diagnosis and corresponding histopathologic diagnosis	46
Table	14	Measures of accuracy for major pre-operative MRI diagnoses	46
Table	15	Patients' symptoms and signs	47
Table	16	Crosstabulation of histopathologic diagnosis and pain as a symptom	48
Table	17	Crosstabulation of histopathologic diagnosis and proptosis as a symptom	49
Table	18	Crosstabulation of histopathologic diagnosis and swelling as a symptom	49
Table	19	Crosstabulation of histopathologic diagnosis and ptosis as a symptom	50

Table	20	Crosstabulation of histopathologic diagnosis and diplopia as a symptom	50
Table	21	Logistic Regression Model: Correct MRI Diagnosis*Clinical signs and symptoms	51
Table	22	MRI findings	53
Table	23	Crosstabulation of histopathologic diagnosis and bone erosion in the MRI	54
Table	24	Crosstabulation of histopathologic diagnosis and perineural invasion in the MRI	55
Table	25	Crosstabulation of histopathologic diagnosis and margins of lesion in the MRI	56
Table	26	Strength of magnetic field	57
Table	27	Different contrast agents used	57
Table	28	Degree of correspondence between pre-operative orbital MRI diagnosis and corresponding histopathologic diagnosis from the different groups of patients	58
Table	29	Variables and their contributions to a logistic Regression Model: Correct MRI Diagnosis*MRI specifications	59
Table	30	Crosstabulation of histopathologic diagnosis and T1-Weighted Image characteristics in the MRI	60
Table	31	Crosstabulation of histopathologic diagnosis and T2-Weighted Image characteristics in the MRI	60
Table	32	Crosstabulation of histopathologic diagnosis and degree of contrast agent’s enhancement in the MRI	61
Table	33	Logistic Regression Model: Correct Diagnosis*MRI findings	62
Table	34	Treatment according to pathologic diagnosis	63
Table	35	Recurrence rates and time until recurrence	64
Table	36	Incidence of PEMLG from reports that listed the number of individual tumors	66

List of Figures

Figure	1	Frontal view of the lacrimal gland	13
Figure	2	Diagrams of the lacrimal glands Types I to III	14
Figure	3	Superior view of the lacrimal gland's arterial vasculature	15
Figure	4	Annulus of Zinn	16
Figure	5	Schematic representation of the tear film	19
Figure	6	Schematic representation of the lacrimal system	21
Figure	7	Example of an MRI of a patient from our cohort, showing a physiological lacrimal gland on the right side and a pleomorphic adenoma on the left side.	30
Figure	8	Representation of the "wedge sign"	31
Figure	9	Distribution of the greatest dimension of lacrimal gland tumors from 72 patients' MRI reports	53

List of Abbreviations

Apparent diffusion coefficient (ADC)

Area under the receiver operating characteristic curve (AUC)

Benign reactive lymphoid hyperplasia (BRLH)

Best corrected visual acuity (BCVA)

Bone morphogenetic protein 7 (Bmp7)

Calcitonin gene-related peptide (CGRP)

Correct Diagnosis (CDx)

Cohen’s kappa coefficient (k)

Confidence Interval (CI)

Contrast agent (CA)

Cytomegalovirus (CMV)

Computed Tomography (CT)

Dynamic contrast enhanced (DCE)

Dry Eye Disease (DED)

Diffusion-weighted imaging (DWI)

Epstein-Barr virus (EBV)

Fast spin-echo (FSE)

Goldmann applanation tonometry (GAT)

Graft-versus host disease (GvHD)

Granulomatosis with polyangiitis (GPA)

Human immunodeficiency virus (HIV)

International Classification of Procedures in Medicine (ICPM)

International Statistical Classification of Diseases and Related Health Problems (ICD)

Immunoglobulin (Ig)

Immunoglobulin G4 (IgG4)

Intra-ocular pressure (IOP)

Magnetic resonance imaging (MRI)

Negative Predictive Value (NPV)

Non-contact tonometry (NCT)

Operationen- und Prozedurenschlüssel (OPS)

Oxygen (O_2)

Primary Epithelial Malignancies of the Lacrimal Gland (PEMLG)

Primary Epithelial Tumors of the Lacrimal Gland (PETLG)

Positive Predictive Value (PPV)

Spin-echo (SE)

Standardized Beta Weight for X (BwX)

Substance P (SP)

Tesla (T)

Thyroid eye disease (TED)

Ultrasonography (US)

Vasoactive intestinal polypeptide (VIP)

World Health Organisation (WHO)

Zusammenfassung

Ziel: In dieser Arbeit wird die präoperativ radiologisch gestellte Verdachtsdiagnose mit dem histopathologischen Befund bei Tränendrüsentumoren verglichen, um die Aussagekraft der Magnetresonanztomographie (MRT) als diagnostisches Mittel für diese Erkrankung zu bewerten. Mittels Kreuztabellen und logistischer Regressionsmodellen sollen zudem Prädikatoren für eine richtige radiologische Diagnose ermittelt werden. Des Weiteren wird die Inzidenzrate der Tränendrüsentumoren in Berlin zwischen 2011 und 2018 berechnet.

Methoden: In unsere monozentrische retrospektive Studie wurden Patienten eingeschlossen, die sich von 1997-2019 mit einem in einer radiologischen Bildgebung diagnostiziertem Tränendrüsentumor in unserer Klinik vorstellten, und eine histopathologische Befundung erhielten. Eine Analyse der klinischen Daten von 112 Patienten sowie eine Zuverlässigkeitsgradberechnung der radiologischen Verdachtsdiagnose mittels Cohen's kappa-, Chi2- und Cramer's V-Tests wurde durchgeführt. Statistische Gütekriterien wurden erhoben. Die Inzidenz wurde berechnet und logistische Regressionsmodelle mit bestimmten Prädiktoren wurden erstellt.

Ergebnisse: Der Übereinstimmungsgrad zwischen radiologischer und histopathologischer Diagnose zeigte eine moderate Zuverlässigkeit k=0.451 (p-value <0.001). Der Übereinstimmungsgrad war bei durchgeführtem 3-Tesla-MRT am Höchsten. Der positive prädikative Wert für die Diagnosen Dakryops und Dakryoadenitis lag bei ca. 80%. Die häufigsten Diagnosen waren Dakryoadenitis (40%) und Lymphom (19%). Klinisch gaben die Patienten am häufigsten eine Lidschwellung an. Es bestand ein statistisch hoher signifikanter Zusammenhang zwischen Proptosis/Schwellung und histopathologischer Diagnose (Cramer's V = 0.45; p-Wert < 0.002). Folgende Zusammenhänge wurden festgestellt: Pleomorphes Adenokarzinom - Schmerzen, Adenoid zystisches Karzinom - Proptosis sowie Dakryoadenitis/ benigner reaktiver lymphoider Hyperplasie - Schwellung. In unserem logistischen Regressionsmodell war das Symptom Lidschwellung ein statistisch signifikanter Prädiktor für eine korrekte radiologische Diagnose. Zudem zeigte sich ein statistisch hoch signifikanter Zusammenhang zwischen den MRT-Merkmalen Knochenerosionen, Tumorränder und perineurale Infiltration und histopathologischer Diagnose gemäß dem Cramer-V-Test. Folgende Zusammenhänge waren ebenso statistisch signifikant: perineurale Infiltration - pleomorphes Adenokarzinom, Knochenerosion - adenoidzystisches Karzinom, T2-isointense spezifische Eigenschaften - Lymphom sowie fehlende Kontrastmittelaufnahme – Dakryops. Die Gesamtinzidenz der Tränendrüsentumore in Berlin betrug 1,93/100.0000/Jahr für den Zeitraum von 2011 bis 2018.

Schlussfolgerungen: Es besteht eine moderate Verlässlichkeit der mittels MRT festgestellte Diagnose eines Tränendrüsentumors. Dabei war der prädikative Wert am höchsten für Dakryops/Dakryoadenitis. Zur weiteren Einordnung dieser Ergebnisse sollten weitere Untersuchungen mit höherer Fallzahl erfolgen.

Abstract

Purpose: The aim of this study is to ascertain the reliability of magnetic resonance imaging as a diagnostic tool for lacrimal gland tumors in a clinical setting, by comparing the diagnosis put forward by radiologists with the post-operative histopathological diagnosis. Furthermore, we will strive to uncover predictors of a correct image-based diagnosis through crosstabulations of the data and logistic regression models. An estimation of the incidence rate of lacrimal gland tumors in Berlin during 2011-2018 is attempted.

Materials and Methods: Patients with a lacrimal gland lesion who presented themselves at our clinic from 1997 to 2019 were identified in this retrospective unicentric study. Those with an image-based tumor diagnosis pre-surgery and pathologic tumor diagnosis post-surgery were included in this study. The degree of reliability of the image-based diagnosis for these 112 patients was computed and their clinical data was analyzed with recourse to Cohen's kappa, Chi-square, and Cramer's V tests. Measures of accuracy were obtained. An incidence rate was calculated. Logistic regression models with selected predictors were performed.

Results: The degree of correspondence between image-based diagnosis and histopathologic diagnosis revealed a moderate agreement of k=0.451 (p-value <0.001). This reliability was higher for MRI examinations carried out with a 3 T magnetic strength field. Dacryops/dacryoadenitis showed a positive predictive value of ca. 80%. The overall crude incidence rate (2011-2018) was 1.93/1,000,000/year. The most common diagnoses were dacryoadenitis (40%) and lymphoma (19%). The chief complaint was swelling (74%), while pain (8%) was the least observed symptom. There was a very strong statistically significant interdependence between proptosis/swelling and pathologic diagnosis (Cramer's V = 0.45; p-value < 0.002). More specifically, the following statistically significant relationships were uncovered: pain with pleomorphic adenocarcinoma, proptosis with adenoid cystic carcinoma, and swelling with dacryoadenitis and with benign reactive lymphoid hyperplasia. Swelling was a statistically significant predictor of a correct image-based diagnosis in our logistic regression model. Furthermore, there was a very strong statistically significant interrelation between all MRI features (bone erosion, margins of lesion and perineural invasion) and pathologic diagnosis according to the Cramer's V test. In detail, the following interdependences were statistically significant: perineural invasion/pleomorphic adenocarcinoma, bone erosion/adenoid cystic carcinoma, T2-isointense internal features/lymphoma and no contrast enhancement/dacryops.

Conclusions: There is a moderate reliability of the MRI diagnosis of lacrimal gland tumors, with the positive predictive value being highest for dacryops/dacryoadenitis. Due to the reduced number of patients in our study, there are limitations in interpreting subgroup results.

1 – Introduction

1.1 Anatomy, Development, and Physiology of the human lacrimal secretory system

1.1.1 Anatomy of the human lacrimal secretory system

The human lacrimal system encompasses the lacrimal gland and the accessory lacrimal glands, which are responsible for the production of the aqueous layer of the tear film.

The typical main lacrimal gland (also called lacrimal gland of Henle and Manz), the major component of the system, can be divided into 2 portions: the orbital and the palpebral. These two are separated by the levator aponeurosis, which itself is composed of the levator muscle's lateral fibers, the lateral rectus muscle's lateral fibers, and the lateral ligamentous winglet of the eyeball's fascial sheath, also known as Tenon's capsule (Rouvière & Delmas, 2005). This bilobed, tear-shaped gland rests on the lacrimal fossa of the frontal bone, located on the upper fronto-temporal orbita, as represented in Figure 1 (Netter, 2018).

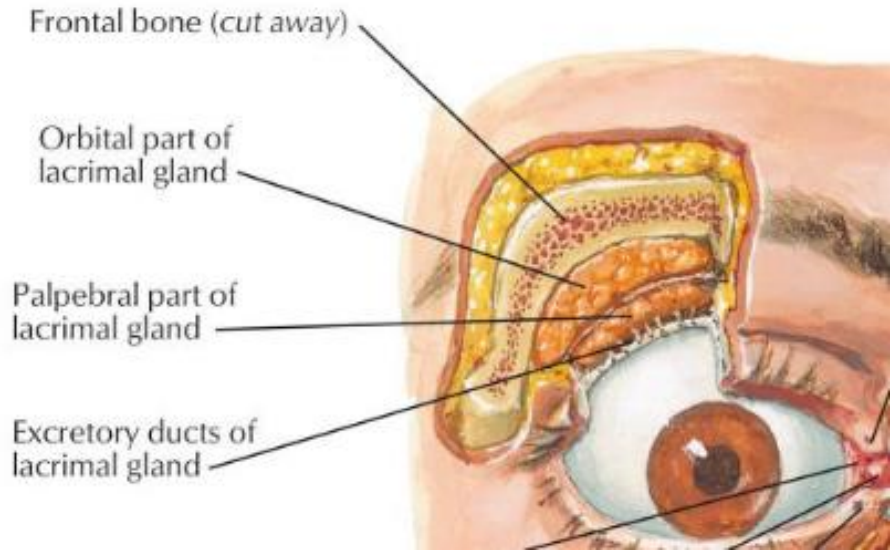

Fig. 1: Frontal view of the lacrimal gland (Netter, 2018)

INTRODUCTION

The lacrimal gland is an exocrine gland in which each lobule is formed by acinar cells, which are surrounded by myoepithelial cells with flattened nuclei. These are capable of contraction via neuronal stimulation, leading to fluid excretion. The gland's excretory ducts transverse the orbital lobe - together with blood vessels, lymphatics and nerves - into the palpebral lobe and progress inferior-nasally until they reach the upper conjunctival fornix. Because of this particular trajectory, biopsies should preferentially be performed on the orbital lobe to try and preserve as much of the normal anatomy as possible (AAO, 2016).

The accessory lacrimal glands are located laterally at the upper fornix (Glands of Krause) and along the margin of both tarsal plates (Glands of Wolfring). They are cytologically identical to the main gland and together they account for only ca. 10% of the total tear secretion (Mausolf, 1975).

Variations of the main lacrimal gland's typical configuration (or Type I) appear to be quite common, as reported by Bock in 1896 (cited in (Duke-Elder, 1961). This was also recognized by Werb (1983), but it was not until the new millennium that these variants were approached with more scientific rigor. In 2009, Lorber and Vidic found 51.1% of the 45 examined glands exhibited a discrepancy from the norm. They described three variants in detail, with the most common one being the subencapsulated or Type II gland (26.7% of the 45 glands), where dense connective or fibro-adipose tissue coats its deep surface, narrowing the interlobar gap and restricting the characteristic movement of its palpebral portion. The Type III or bilayered variant describes the situation where the orbital lobe sits on top of the palpebral one (22.2%). The macrovariant or Type IV represents the last variant, which was observed in only one specimen (2.2%), where both lobes are of greater dimensions. A diagram of these variants is shown in Figure 2 (Lorber & Vidic, 2009; Werb, 1983).

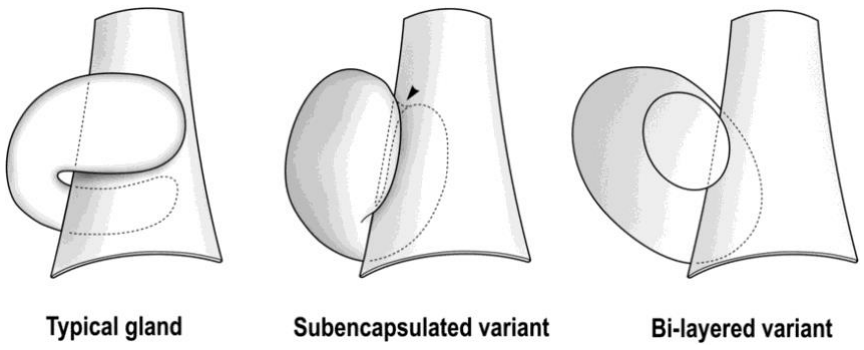

Fig. 2: Diagrams of the lacrimal glands Types I to III (Lorber & Vidic, 2009)

There are known gender differences in size and weight as well. The male lacrimal gland averages 22.04 mm ± 2.28 in width, 18.88 mm ± 2.43 in depth and 1.34 g ± 0.27 in weight, exceeding the female one in all measurements (19.93 mm ± 2.07; 17.08 mm ± 2.84; 0.96 g ± 0.30, respectively) (Duke-Elder, 1961). This sexual dimorphism can be partly explained as due to the fact that the lacrimal gland is a target organ for androgens, as shown by numerous animal studies which documented the presence of high-affinity receptors for androgens, but not estrogens, in the rabbit/rat lacrimal gland (Krawczuk-Hermanowiczowa, 1983; Sullivan, Edwards, Wickham, Pena, Gao, Ono, & Kelleher, 1996).

Furthermore, the higher concentration of androgens in the blood stream of men accounts not only for this morphological difference between genders, but also for a functional one, since the tear secretion may be reduced at a low concentration of androgens, which helps explain the predominance of dry eye disease in women (Azzarolo, Mircheff, Kaswan, Stanczyk, Gentschein, Becker, Nassir, & Warren, 1997).

Blood reaches the eye and the main lacrimal gland through the ophthalmic artery, which itself stems from the internal carotid artery, branching next to the optic chiasm and following along the optic nerve until its division into three groups. The first group branches inferior and laterally to the optic nerve, giving way to the central retinal artery

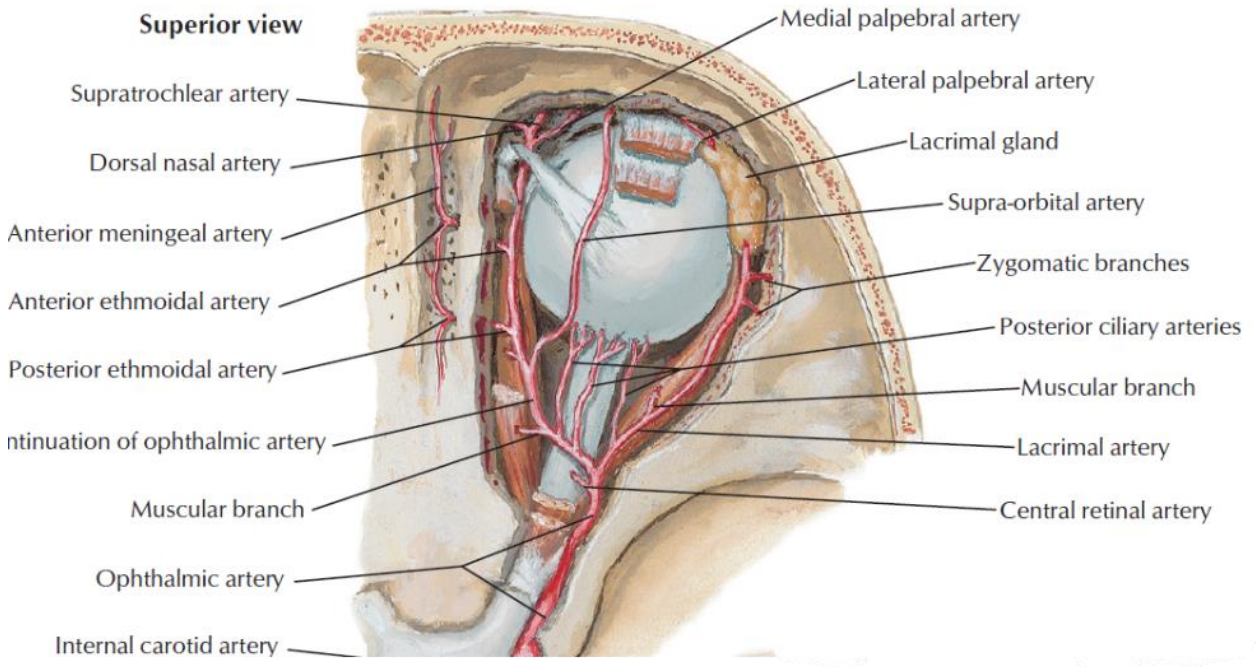

Fig. 3: Superior view of the lacrimal gland's arterial vasculature (Netter, 2018)

and to the lacrimal artery. The lacrimal artery follows antero-laterally along the upper border of the lateral rectus muscle until it meets the lacrimal gland. The zygomatic branches also originate from it. The other two groups of the ophthalmic artery are responsible for the remaining vessels pictured in Figure 3 (Netter, 2018; Rouvière & Delmas, 2005).

In turn, the lacrimal vein drains blood from the lacrimal gland and continues posteriorly into the superior ophthalmic vein, which itself anastomoses with the inferior ophthalmic vein, passing through the superior orbital fissure laterally to the annulus of Zinn and culminating at the cavernous sinus. All these veins are absent of valves (Rouvière & Delmas, 2005).

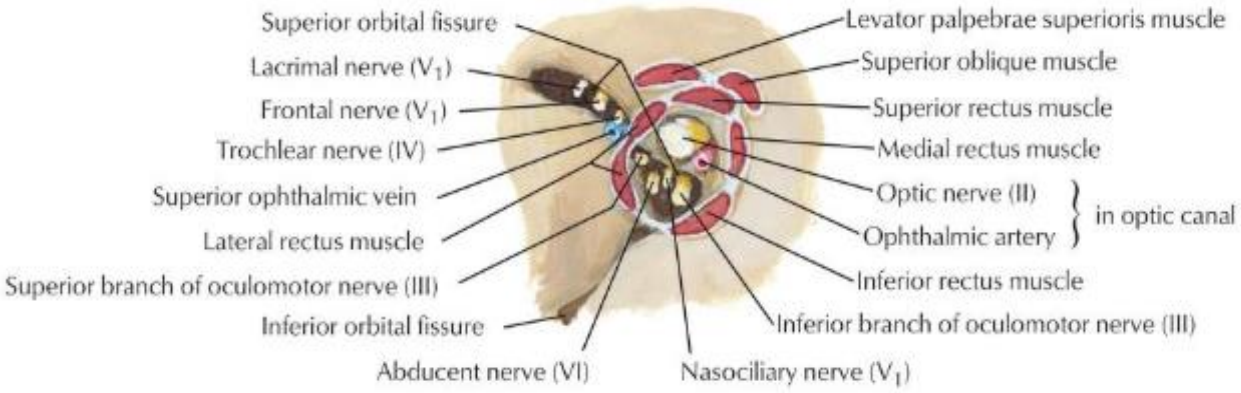

Fig. 4: Annulus of Zinn (Netter, 2018)

The main lacrimal gland is innervated by parasympathetic and sympathetic nerves, which stimulate the lacrimal gland's secretion, as well as some sensory nerves.

The parasympathetic nerves originate in the lacrimal nucleus of the facial nerve (VII) in the cerebral pons, forming the greater petrosal nerve at the geniculate ganglion, which then combines with the deep petrosal nerve, forming the nerve of the pterygoid canal (of Vidian) and end up synapsing on the pterygopalatine ganglion. From here, the most recent study on the matter (Scott, 2014) shows that the postsynaptic fibers branch into the zygomatic and zygomatico-temporal nerves. The zygomatico-temporal nerves then reach the lacrimal gland directly ca. 60% of the time, as opposed to via the normal pathway described in anatomy textbooks. They communicate with the lacrimal nerve in only ca. 30% of cases, in addition to having the direct connection to the lacrimal gland. However, another study (Ruskell, 2004) showed that the lacrimal

gland may receive its parasympathetic nerves directly from the retro-orbital plexus (Ruskell, 2004; Rusu, 2010; Scott, Balsiger, Kluckman, Fan, & Gest, 2014).

The sympathetic nerves originate in the superior cervical ganglion and travel alongside the internal carotid artery, continuing as the deep petrosal nerve until they are part of the nerve of the pterygoid canal. However, these postsynaptic fibers do not synapse on the pterygopalatine ganglion. Instead, they simply progress further into the lacrimal gland.

The ophthalmic nerve represents the first ramification of the trigeminal nerve at the trigeminal ganglion (of Gasser). It travels on the lateral wall of the cavernous sinus, originating several terminal branches: the nasociliary nerve, the frontal nerve and the lacrimal nerve. The latter travels antero-laterally through the superior orbital fissure, as seen in Figure 4 (laterally to the annulus of Zinn with the frontal and trochlear nerve), next to the lacrimal artery, reaching the lacrimal gland, where it gives off several filaments supplying sensory innervation to the gland and conjunctiva. It then perforates the orbital septum to culminate in the skin of the upper eyelid. On some occasions the lacrimal nerve is absent, so that the sensory innervation of the gland is substituted by the zygomatico-temporal branch of the maxillary nerve (Rouvière & Delmas, 2005).

The parasympathetic neurotransmitters involved are vasoactive intestinal polypeptide (VIP) and acetylcholine, whereas the sympathetic neurotransmitters are neuropeptide Y (NPY) and norepinephrine. The sensory innervation contains substance P (SP) and calcitonin gene-related peptide (CGRP). The accessory lacrimal glands are also richly innervated, containing VIP, substance P, and CGRP (Botelho, Hisada, & Fuenmayor, 1966; Sibony, Walcott, McKeon, & Jakobiec, 1988).

To date, the lymphatic system of the orbit and lacrimal gland is still poorly understood (Sherman, Gonnering, Wallow, Lemke, Doos, Dortzbach, Lyon, & Bindley, 1993).

1.1.2 Development of the human lacrimal secretory system

The embryology of the human lacrimal gland is a complex process and an area of ongoing research. It encompasses cells from immune, epithelial and mesenchymal lineages, with their interaction playing a crucial part in the formation of viable glands (D. J. T. Farmer, Nathan, Finley, Shengyang Yu, Emmerson, Byrnes, Sneddon, McManus, Tward, & Knox, 2017).

Its morphogenesis can be divided in three phases: presumptive glandular stage; epithelial bud stage; and glandular maturity stage. The epithelial bud stage takes place at the end of the embryonic period, starting between the sixth and seventh weeks of gestation, with buds arising from solid chords of epithelial cells of the temporal region of the superior conjunctival fornix through vacuolation and development of lumina. Five or six of them ultimately form the orbital lobe of the human lacrimal gland and subsequently new buds start forming in order to develop the palpebral lobe (de la Cuadra-Blanco, Peces-Peña, & Mérida-Velasco, 2003; del Castillo, 1981; Frederick A Jakobiec, 1982).

The branching of buds into terminal ductule lobular units was shown to be regulated by bone morphogenetic protein 7 (Bmp7) through signaling via the mesenchymal lineage (Dean, Ito, Makarenkova, Faber, & Lang, 2004).

The glandular maturity stage occurs from the ninth week onwards, already during the fetal period. Eyelid appendages, the levator palpebrae superioris and pilosebaceous units develop between the third and sixth months. At birth, the lacrimal glands are still small. Tear secretion only begins three weeks or more after birth. Thus, newborn infants cry without tears (Duke-Elder, 1970; Moore & Persaud, 2008).

1.1.3 Physiology of the human lacrimal secretory system

1.1.3.1 The human tear film and its secretion

The human tear film can be divided in three compartments: the fornical, the tear menisci, and the preocular (Willcox, Argüeso, Georgiev, Holopainen, Laurie, Millar, Papas, Rolland, Schmidt, Stahl, Suarez, Subbaraman, Uçakhan, & Jones, 2017). The preocular tear film can in turn be further distinguished as prebulbar and precorneal, the latter representing a vital part in the maintenance of a healthy eye surface by enabling comfortable and sharp vision. Modern research shows it to be 2-5 µm thick, with a mean pH value range of 6.8 to 8.2, and composed of three usually stable layers, listed below and represented in Figure 5 (Chen, Wang, Tao, Shen, Jiao, & Lu, 2010; Holly & Lemp, 1977; King-Smith, Fink, Hill, Koelling, & Tiffany, 2004; Wolff, 1946):

1 – a superficial oily layer;

2 – an aqueous layer;

3 – a deep mucin layer.

The first layer is made of meibum, that is, a mix of polar (phospholipids) and non-polar (cholesterol, wax esters, cholesterol esters) lipids and proteins, which is secreted during lid movement into the eyelid margin at the mucocutaneous junction by the meibomian glands. These are sebaceous holocrine glands of acino-tubular structure and parasympathetic innervation located in the tarsal plate of both upper and lower eyelids (Foulks & Bron, 2003). Their main function is to confer stability and durability to the tear film, preventing the rapid evaporation of the aqueous layer through a decrease of the surface tension at the air interface (Nichols, Foulks, Bron, Glasgow, Dogru, Tsubota, Lemp, & Sullivan, 2011; Peng, Cerretani, Li, Bowers, Shahsavarani, Lin, & Radke, 2014).

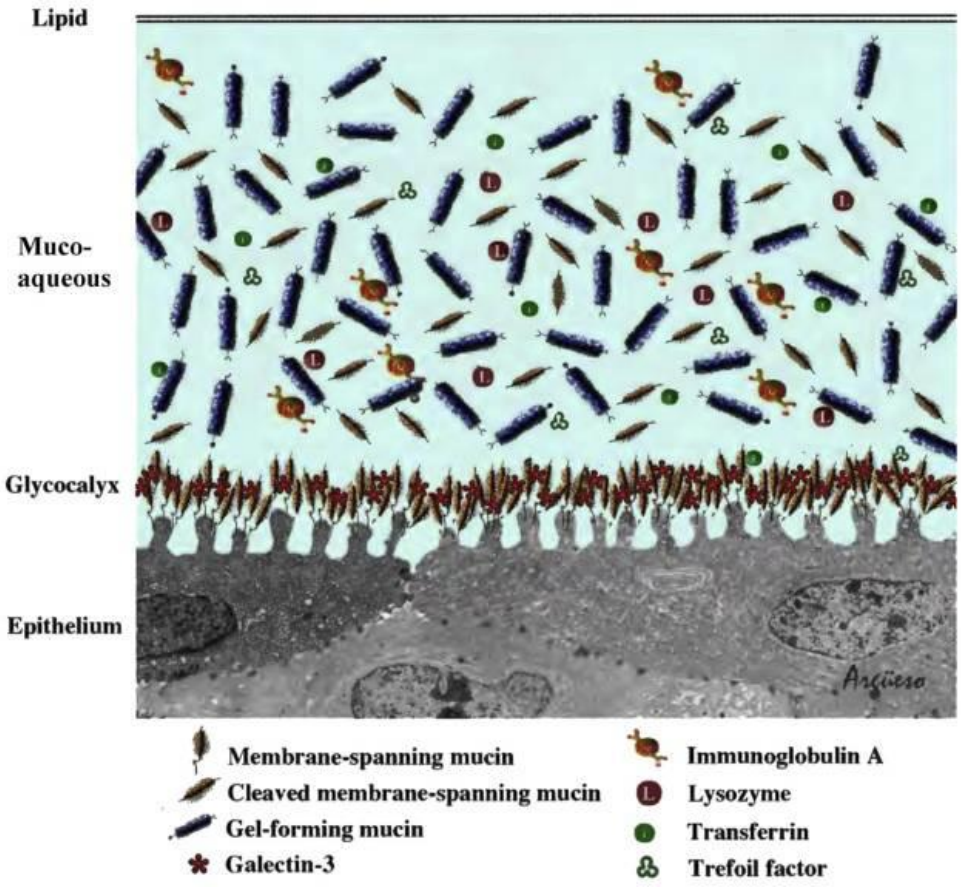

Fig. 5: Schematic representation of the tear film (adapted from Willcox, Argüeso, Georgiev, Holopainen, Laurie, Millar, Papas, Rolland, Schmidt, Stahl, Suarez, Subbaraman, Uçakhan, & Jones, 2017)

INTRODUCTION

The middle aqueous layer represents the main component of the tear film. It serves several purposes, such as: lubrication of the exposed ocular surface, maintenance of appropriate tear osmolarity, protection through anti-microbial and anti-viral proteins (e.g.: Immunoglobulin A, lactoferrin, lysozyme, defensins, interferon, etc.), and providing nutrients and oxygen to the avascular corneal epithelium (Willcox, Argüeso, Georgiev, Holopainen, Laurie, Millar, Papas, Rolland, Schmidt, Stahl, Suarez, Subbaraman, Uçakhan, & Jones, 2017). The main lacrimal gland is the major agent involved in its secretion, which occurs at a base rate of 8 ± 3 µL (Kuppens, Stolwijk, de Keizer, & van Best, 1992; Mishima, Gasset, Klyce, & Baum, 1966). Nonetheless, in its absence, the eye is still able to maintain a lubricated ocular surface through the supporting accessory lacrimal glands and conjunctival epithelia (Dartt, 2002; Stevenson, Pugazhendhi, & Wang, 2016).

The deep mucin layer is mostly secreted by the conjunctival and corneal epithelia with the main lacrimal gland having a minimal role. Mucins are multifunctional molecules composed of negatively-charged, high-molecular-weight glycoproteins, which protect the corneal epithelial cells against infection and injury. It also lowers the corneal hydrophobicity, providing a better and more uniform adherence for the tear film (Gipson & Argueso, 2003; Govindarajan & Gipson, 2010).

Thus, tear secretion represents a complex physiological process which is influenced by a myriad of factors and governed via the cornea–trigeminal nerve–brain-stem–facial nerve–lacrimal gland reflex arc. It is usually classified into four types: basal, emotional, reflex and closed-eye. The basal secretion, also known as open-eyed secretion, represents the standard situation, where tears are continually produced to wet the ocular surface at a rate between 1 to 3.4 µL/min and a volume of 7 µL (Eter & Gobbels, 2002; Kuppens, Stolwijk, de Keizer, & van Best, 1992; Paulsen, Schaudig, & Thale, 2003). An increase due to emotions would represent the emotional type, where as an increase due to physical irritation (sensory stimulation of the ophthalmic branch of the trigeminal nerve), intense light, or psychogenic factors would represent the reflex type. Lastly, closed-eye secretion represents what happens during sleep (Tan, Sack, Holden, & Swarbrick, 1993).

These four types differ not only in quantity of secretion, i.e., flow rate, but also in quality, since the composition of tears has long been known to be different. For

example, Immunoglobulin (Ig) M and A concentrations decrease with an increase in flow rate (Fullard & Snyder, 1990; Fullard & Tucker, 1994; Fullard & Tucker, 1991).

The lacrimal tears follow a downward and inward path from the lacrimal gland, making their way through the cornea to the lacrimal ducts, from which they finally reach the nasolacrimal duct, as can be seen in Figure 6 below (Stein, 2012).

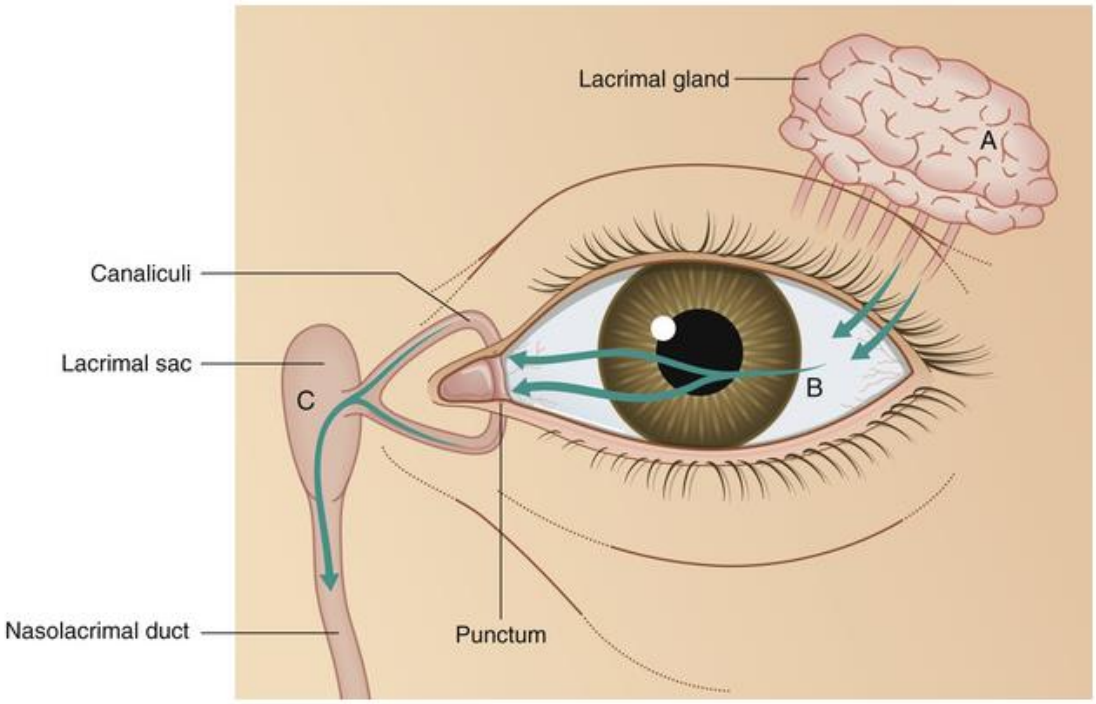

Fig. 6: Schematic representation of the lacrimal system (Stein, 2012)

1.2 Clinicopathology of the human lacrimal gland

Congenital pathologies of the human lacrimal gland are extremely rare. Some, like aplasia and hypoplasia, appear to follow an autosomal dominant pattern (AAO, 2016; Kim, Hwang, Kweon, Kim, & Oh, 2005). Lacrimal fistulas, and ectopic and prolapsed lacrimal glands have also been reported (Morandi, Valerio, & Cutrone, 2016; Nagendran, Alsamnan, Strianese, & Malhotra, 2020).

Tumors of the human lacrimal gland share similarities to those of the major salivary glands and are rare, which hinders a comprehensive population-based study. As a result, their reported incidence varies widely in the literature (J. A. Shields, Bakewell, Augsburger, & Flanagan, 1984). The latest estimate puts it at 1.3/1,000,000 per year (S. L. von Holstein, Coupland, Briscoe, Le Tourneau, & Heegaard, 2013).

Broadly, they comprise 5 to 25% of all orbital space-occupying tumors and are found in patients across all ages, but are mostly a disease of middle-aged adults without any racial predilection (Frederick A Jakobiec, 1978; Ni, Kuo, & Dryja, 1992; Seregard & Sahlin, 1999; C. L. Shields, Shields, Eagle, & Rathmell, 1989; Sunderraj, 1991; S. L. von Holstein, Coupland, Briscoe, Le Tourneau, & Heegaard, 2013; Weis, Rootman, Joly, Berean, Al-Katan, Pasternak, Bonavolontà, Strianese, Saeed, Feldman, Vangveeravong, Lapointe, & White, 2009). Moreover, an epidemiological study from Japan revealed a gender bias for some types of lacrimal gland tumors ("An epidemiological survey of lacrimal fossa lesions in Japan: number of patients and their sex ratio by pathological diagnosis," 2005).

A hallmark of these lesions are their variable array of symptoms like proptosis, infero-nasal displacement of the globe, pain, restriction of motility, diplopia, ptosis, bone destruction, and eventually reduced visual acuity (J. A. Shields & Shields, 2008).

In the past, some authors proposed a classification into four groups according to their frequency (from most frequent to least): inflammatory, lymphoid, metastatic and primary epithelial (Font, Smith, & Bryan, 1998; Paulino & Huvos, 1999).

Nowadays, however, a differentiation according to their origin is conventionally applied, so that they can be divided chiefly into 2 categories: epithelial (ca. 20%), also known as primary epithelial tumors of the lacrimal gland (PETLG), and non-epithelial lesions (ca. 80%) (J. A. Shields & Shields, 2008).

Together, they encompass a myriad of disorders, the more frequent being depicted in Table 1, along with their observed incidence on a survey of 1,264 orbital tumors, where 114 or 9% of the total were lacrimal gland lesions (J. A. Shields, Shields, & Scartozzi, 2004). Some authors choose to exclude the purely cystic lesions, i.e., dacryops, bringing the ratio of epithelial to non-epithelial lesions closer to the aforementioned 20/80%.

Table 1. Lesions of the human lacrimal gland and their incidence

Epithelial	
Dacryops	17%
Adenoid cystic carcinoma	12%
Pleomorphic adenoma	10%
Pleomorphic adenocarcinoma	4%
Mucoepidermoid carcinoma	1%
Non-Epithelial	
Dacryoadenitis	33%
Non-Hodgkin's Lymphoma	14%
Benign reactive lymphoid hyperplasia	6%
Atypical lymphod hyperplasia	1%
Plasmacytoma	1%
Lymphoepithelial hyperplasia	1%

With regards to the epithelial lesions, ca. 55% are benign and can be differentiated into dacryops, pleomorphic adenoma, acidophilic cytoma and squamous adenoma (J. A. Shields, 1989).

The remaining 45% are malignant and are also known as primary epithelial malignancies of the lacrimal gland (PEMLG). Their average incidence is represented in Table 2, with adenoid cystic carcinoma representing 65% of the total, as derived from a complex review of English-language literature by Shields et al. (J. A. Shields, C. L. Shields, J. A. Epstein, R. Scartozzi, & R. C. Eagle, Jr., 2004).

Table 2. Types of PEMLG and their incidence

Adenoid cystic carcinoma	63%
Pleomorphic adenocarcinoma	19%
De novo adenocarcinoma	10%
Mucoepidermoid carcinoma	4%
Squamous cell carcinoma	2%
Sebaceous cell carcinoma	1%
Acinic cell carcinoma	1%
Ductal carcinoma	<1%
Lymphoepithelial carcinoma	<1%
Basal cell carcinoma	<1%
Myoepithelial carcinoma	<1%
Cystadenocarcinoma	<1%

1.2.1 Benign primary epithelial tumors of the lacrimal gland

The most common benign PETLG are pleomorphic adenoma and dacryops, which exhibit no bone destruction and are usually painless (J. A. Shields, Shields, & Scartozzi, 2004).

Pleomorphic adenoma, also known as benign mixed tumor, presents as a slow-growing unilateral mass and should always be excised in toto, as a breach of its pseudocapsule (compressed remnants of the surrounding healthy tissue) may lead to recurrence and/or malign transformation into a pleomorphic adenocarcinoma, even decades later (J. A. Shields & Shields, 1987). Therefore, a high-degree of suspicion should be held at the time of examination (Reese, 1956; Rose & Wright, 1992; Stewart, Krohel, & Wright, 1979; Wright, Stewart, & Krohel, 1979).

Dacryops, or ductal epithelial cyst, is a non-tender and mobile mass which results from the occlusion of the lacrimal gland's ducts and can be either unilateral or bilateral. It can resolve on its own or remain stable for a long period of time without surgery (Smith & Rootman, 1986).

1.2.2 Primary epithelial malignancies of the lacrimal gland

Adenoid cystic carcinoma is the most prevalent malign PETLG or PEMLG, with pain being its cardinal symptom. This occurs due to perineural invasion, so that the presence of hypesthesia of the cheek and peri-orbital region should be tested (J. A. Shields & Shields, 2008). It usually progresses faster than benign lesions, invades surrounding structures, and has a high rate of recurrence despite therapy; thus, it is known to have a poor outcome, although young patients may have a more favorable prognosis (Tellado, McLean, Specht, & Varga, 1997).

Some cases were reported where the adenoid cystic carcinoma occurred away from its usual supero-lateral location in the orbit, possibly arising from an ectopic lacrimal gland or from the accessory lacrimal glands at the conjunctival fornix (Duke, Fahy, & Brown, 2000; J. A. Shields, Shields, Eagle, Adkins, & De Potter, 1997).

It can be divided in different histopathologic subtypes, such as: cribriform (Swiss cheese), sclerosing, comedo carcinoma, tubular, and basaloid (Font, Smith, & Bryan, 1998).

To date, a consensus on the course of therapy remains elusive (Bartley & Harris, 2002).

The second most common PEMLG is the pleomorphic adenocarcinoma, also known as malign mixed tumor, which can occur as a spontaneous transformation from a pleomorphic adenoma or as a result from its incomplete resection (J. A. Shields, C. L. Shields, J. A. Epstein, R. Scartozzi, & R. C. Eagle, Jr., 2004). It exhibits a high rate of local recurrence, as well as a predisposition to metastasize, often leading to the initial diagnosis of a bone metastasis before the primary tumor is known (Henderson & Farrow, 1980; Waller, Riley, & Henderson, 1973).

1.2.3 Non-Epithelial lesions of the lacrimal gland

1.2.3.1 Dacryoadenitis

The most frequent non-epithelial lesion is the dacryoadenitis, an inflammation of the lacrimal gland which typically causes a discomfort in the region, with severe cases leading to swelling, redness, tenderness, and occasionally, pain (Witmer, 2009).

It can be uni- or bilateral, with some etiologies (e.g.: auto-immune) being more prone to affect both sides simultaneously. Its diverse etiology is portrayed in Table 3 (Gordon, 2006; Ophthalmology, 2016).

Table 3. Etiology of dacryoadenitis

Infectious:
Viral (EBV, HIV, CMV, Hep. C)
Bacterial (Streptococcus, Staphylococcus, Mycobacterium)
Fungal (Zygomycosis, Aspergillosis)
Parasitic (Echinococcosis, Cysticercosis)
Auto-Immune:
Immunoglobulin G4 (IgG4)-related disease
Sjögren's Syndrome
Thyroid eye disease (TED)
Chronic graft-versus host disease (GvHD)
Granulomatous:
Sarcoidosis
Vasculitis:
Granulomatosis with polyangiitis (GPA)
Polyarteritis nodosa
Idiopathic:
Orbital pseudotumor

The infections can be subdivided into 2 groups: acute suppurative dacryoadenitis and chronic dacryoadenitis. The former is usually caused by bacteria, with a more severe and abrupt onset, while the latter, often caused by viruses, has a more protracted development (Foster, Kraus, & Custer, 2003). Viruses are thought to be the most common infectious cause of dacryoadenitis in general (Obata, Yamagami, Saito, Sakai, & Tsuru, 2003; Rhem, Wilhelmus, & Jones, 2000).

The remaining etiologies can be categorized under “Inflammation”, this being the most common cause of dacryoadenitis (Witmer, 2009). Among them we find the orbital

pseudotumor, or idiopathic orbital inflammatory disease of the lacrimal gland, a diagnosis of exclusion which is characterized by an acute onset and by responding well to a high-dose corticosteroid therapy (Weber, Romo, & Sabates, 1999).

1.2.3.2 Lymphoproliferative lesions of the lacrimal gland

Lymphoproliferative lesions represent a widely variable group of diseases, ranging from low-grade lymphoid hyperplasia to highly malignant lymphoma (Knowles, Jakobiec, McNally, & Burke, 1990). They can be a part of systemic disease (ca. 50% of the time) or confined to the orbit (Cockerham & Jakobiec, 1997; Holly & Lemp, 1977; Liesegang, 1993). They are more common in older patients, and usually progress slowly, painless and bilaterally. As such, their diagnosis at an early stage may pose a problem. A thorough examination of the conjunctiva and uvea is crucial, since a "salmon patch" infiltration is typical of this disease (J. A. Shields & Shields, 2008).

The most common is Non-Hodgkin's lymphoma of B-cell lineage and its precursor, benign reactive lymphoid hyperplasia (BRLH) (incidences depicted in Table 1). Together, they account for over 90% of lymphomas affecting ophthalmological regions, for 5% to 14% of all extra-nodal lymphomas, and for 14-24% of all orbital neoplasia, being more frequent in immunosuppressed patients (H. Demirci, Shields, Shields, Honavar, Mercado, & Tovilla, 2002; J. P. Farmer, Lamba, Lamba, Jordan, Gilberg, Sengar, Bence-Bruckler, & Burns, 2005; J. A. Shields, Shields, & Scartozzi, 2004; White, 2019). Their histopathological differentiation usually requires immunohistochemistry and/or flow cytometry, since the scarce tissue retrieved from the biopsy makes it difficult to classify small lymphocytic infiltrates as benign or malign (Higgins, Blankenship, & Kinney, 2008).

While there are around 40 histological subtypes of mature B-cell neoplasms, the most common are represented in Table 4 (Ferry, Fung, Zukerberg, Lucarelli, Hasserjian, Preffer, & Harris, 2007; W. M. Hassan, M. S. Bakry, H. M. Hassan, & A. S. Alfaar, 2016; Olsen & Heegaard, 2019).

Table 4. Common ocular adnexal lymphomas and their incidence

Extranodal marginal zone lymphoma	59%
Diffuse large B-cell-lymphoma	23%
Follicular lymphoma	9%
Mantle cell lymphoma	5%
Small lymphocytic lymphoma/Chronic lymphocytic leukemia	<4%

Their management is undertaken by the Oncology Department, since it is an individualized and complex process supervised by a specialist according to evidence-based guidelines such as the current 2016 revision of the World Health Organization's classification of lymphoid neoplasms (Swerdlow, Campo, Pileri, Harris, Stein, Siebert, Advani, Ghielmini, Salles, & Zelenetz, 2016; White, 2019).

1.3 Imaging of the human lacrimal gland

The human lacrimal gland can be studied through highly developed imaging procedures, such as: ultrasonography (US), computed tomography (CT) and magnetic resonance tomography (MRI).

US uses a high-frequency probe for the orbit (7.5 to 8 MHz) or for the globe (10 MHz), and is useful in distinguishing cystic from solid lesions (Lieb, 1998).

Computed tomography offers a high-resolution and best view of bony anatomy, which explains its relevance in examining the lacrimal gland, on account of its location being partly encased in bone and surrounded by low-density fat. One disadvantage, however, is the exposure to irradiation (Hughes & Miszkiel, 2006).

Nevertheless, nowadays the preferred imaging method of the human lacrimal gland is MRI, which produces images by using strong magnetic fields and radio waves (Mafee, Edward, Koeller, & Dorodi, 1999). The lack of ionizing radiation and the high contrast resolution of the images, with an emphasis on soft-tissue, are some of the benefits which make its use more desirable, especially in younger patients. However, there are some trade-offs as well, such as: greater cost, increased duration of examination, exclusion of patients with non-removable ferromagnetic material in the body, susceptibility to motion artifacts, lower sensitivity for calcification and poorer representation of bony anatomy (Hesselink & Karampekios, 1996; Hornblass, Friedman, & Yagoda, 1981).

Furthermore, in order to increase its signal-to-noise ratio at the expense of a wider field of view, surface coils are recommended in ocular MR-imaging, with a quantitative analysis advancing the use of a 6 cm loop surface coil as the best choice (Erb-Eigner, Warmuth, Taupitz, Bertelmann, Hamm, & Asbach, 2013; Georgouli, Chang, Nelson, James, Tanner, Shelley, Saldana, & McGonagle, 2008; Georgouli, James, Tanner, Shelley, Nelson, Chang, Backhouse, & McGonagle, 2008; Kneeland & Hyde, 1989).

Typical MRI-sequences of the orbit and lacrimal gland include: short spin-echo (SE) T1-weighted sequences (TR 500 to 800ms, TE 12ms) in both axial and coronal planes; a T2-weighted fast spin-echo (FSE) sequence (TR 3400 ms, effective TE 102ms, 16-echo train length) in the axial plane with fat suppression; and post-contrast agent (CA)

axial and coronal T1-weighted images with fat suppression, which improves image quality by revealing further details which would otherwise be obscured by the high signal return of orbital fat (Hughes & Miszkiel, 2006). In addition, the image quality can also be improved by doubling the magnetic field strength to 3 Tesla (T) (Mafee, Rapoport, Karimi, Ansari, & Shah, 2005).

Furthermore, other sequences have been developed, such as diffusion-weighted imaging (DWI) and dynamic contrast enhanced (DCE), which offer some further insight, distinguishing lesions based on their cellularity and vascularity, respectively. High tissue cellularity causes a high restriction of water molecules in the tissue, which leads to a lower apparent diffusion coefficient (ADC) value, making malignancy more likely. Regarding DCE, it has been observed that benign lesions demonstrate a persistent vascularity pattern, while malignant lesions exhibit a washout pattern and higher objective DCE parameters (Lope, Hutcheson, & Khademian, 2010; Ro, Asbach, Siebert, Bertelmann, Hamm, & Erb-Eigner, 2016; Yuan, Kuai, Chen, & Tao, 2013).

Due to its complexity and high number of anatomical structures, the orbit and its contents are divided in 5 compartments. These are: extra-conal, which is the space within the orbit outside the musculofascial cone, limited anteriorly by the orbital septum and exteriorly by the orbital bones; intra-conal, the space internal to the musculofascial cone and limited anteriorly by the posterior half of the globe; the optic nerve; the lacrimal gland; and the bulbus itself (Lemke, Hosten, Foerster, & Felix, 2001).

The normal lacrimal gland is of moderate, sometimes heterogeneous, signal intensity on T1-weighted images and enhances following intravenous contrast agent administration (Hughes & Miszkiel, 2006), as seen in Figure 7, which shows a physiological lacrimal gland on the right side and a pleomorphic adenoma on the left side.

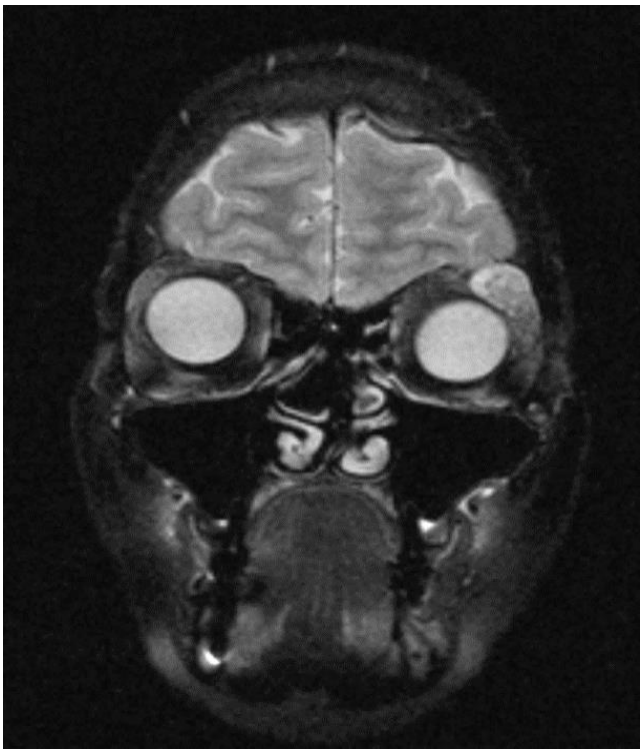

Fig. 7: Example of an MRI of a patient from our cohort, showing a physiological lacrimal gland on the right side and a pleomorphic adenoma on the left side.

INTRODUCTION

The usual standard imaging characteristics presented by the most common lesions of the human lacrimal gland are shown in Table 5 (adapted from Pieper & Thomas, 2014).

Table 5. Standard imaging characteristics of lesions of the human lacrimal gland

Tumor	**MRT-T1**	**MRT-T2**	**MRT with CA**
Epithelial:			
Dacryops	Hypointense	Hyperintense	Peripheral enhancement
Pleomorphic adenoma	Hypo-/Isointense	Iso-/Hyperintense	Moderate, Heterogenous
Adenoid cystic carcinoma	Hypo-/Isointense	Iso-/Hyperintense	Moderate
Non-Epithelial:			
Dacryoadenitis	Hypointense	Hyperintense	Strong, Homogenous
Lymphoma	Isointense	Iso-/Hyperintense	Moderate, Wash-out in late phase

Some other characteristics are highly indicative of a certain type of tumor and/or malignancy. For example, adenoid cystic carcinoma usually causes bone erosion in its later stages, while this occurs at an earlier stage in pleomorphic adenocarcinoma; calcifications are suggestive of malignancy, though not pathognomonic (they may also be observed with choristomas and dermoid cysts); the “wedge sign”, i.e., the presence on MRI/CT of a triangle-shaped tissue between the lateral rectus and lateral orbital wall and the superior rectus and the orbital roof, is more indicative of malignancy (such as adenocarcinoma or lymphoma) in detriment of inflammation (dacryoadenitis), as seen in Figure 8 (Karatza, Shields, Shields, & Eagle, 2004; Lorenzano & Rose, 2017; J. A. Shields & Shields, 2008; Vaidhyanath, Kirke, Brown, & Sampath, 2008).

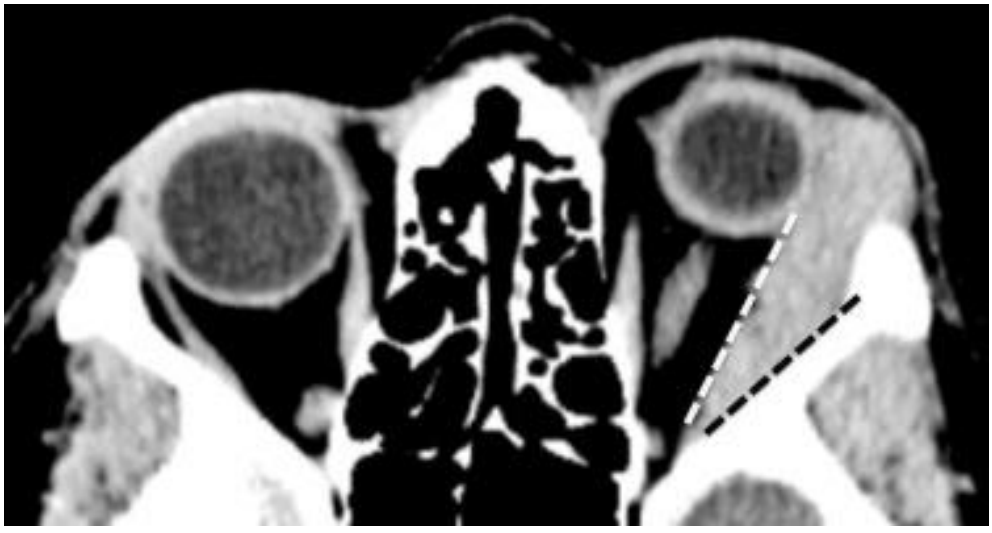

Fig. 8: Representation of the “wedge sign” (Lorenzano & Rose, 2017)

Nevertheless, there is still a high degree of overlap in these standard imaging characteristics between benign and malignant lacrimal gland lesions, to the extent that an accurate diagnosis is often not achieved (Gunduz, Shields, Gunalp, & Shields, 2003; Mafee, Edward, Koeller, & Dorodi, 1999). Multi-parametric MR-imaging with new sequences such as DWI and DCE represent a complementary tool, improving the accuracy of the diagnosis (Razek, Elkhamary, & Mousa, 2011; Ro, Asbach, Siebert, Bertelmann, Hamm, & Erb-Eigner, 2016; Yuan, Kuai, Chen, & Tao, 2013; Zhang, Sha, Qian, Huang, Li, Wang, & Ye, 2014).

1.4 Purpose of this thesis

When working on the diagnosis of a human lacrimal gland tumor, the clinician's most important task is to gather as much information as appropriate in order to recommend a commensurate course of therapy, in case one is required. This process commences at medical university through studying and researching medical books and journals, but that is just the beginning. In the clinical practice, one should not have pre-formed ideas, since each case is different. The first step remains taking a comprehensive medical history and performing an objective examination. From this, an experienced clinician may in some cases promptly advance a first-line diagnosis, with a varying degree of certainty. However, due to the fact that tumors of the human lacrimal gland hide themselves from naked-eye observation and palpable examination, in order to be able to ascertain the true extent of the lesion and its nature, imaging diagnostic tools are usually utilized (Ophthalmology, 2016).

Its disadvantages notwithstanding (e.g., greater cost, less availability, etc.), magnetic resonance imaging is the gold-standard imagiological tool for the diagnosis of lacrimal gland tumors (Mafee, Edward, Koeller, & Dorodi, 1999). Responsible clinicians should avail themselves of this examination, since a correct diagnosis is of the utmost importance. This is clearly understandable in light of the fact that some malignant tumors (e.g., adenoid cystic carcinoma) require a swift excision, lest they metastasize, causing a premature death in some patients, whereas other lesions (e.g., dacryoadenitis) should be treated conservatively instead. To distinguish between malignant and benign lacrimal gland lesions is not sufficient, since some malignant lesions (e.g., lymphoma) can call for biopsy and adjuvant therapy in the form of radiotherapy or chemotherapy, while others (e.g., pleomorphic adenoma) call for a complete and delicate excision, without breach of the involving capsule, to prevent recurrence (J. A. Shields & Shields, 2008; Swerdlow, Campo, Pileri, Harris, Stein, Siebert, Advani, Ghielmini, Salles, & Zelenetz, 2016; White, 2019).

To drive the point home, tumors of the human lacrimal gland are difficult to diagnose/differentiate, which is why an MRI is required. And since the tumors themselves are treated and respond to treatment differently, a correct MRI-based diagnosis is indispensable. Which is why the main purpose of this study will be to

assess if MRI-based diagnoses for lacrimal gland lesions can be relied upon, this being our primary outcome, and if so, with how much certainty. To achieve this, we will compare the pre-operative MRI-diagnosis put forward by radiologists with the post-operative histopathologic findings from patients in our hospital over the last 22 years.

After calculating the overall reliability of the pre-operative MRI diagnosis, we will try to uncover groups of patients which achieve a higher value of reliability, based on several factors (e.g., diagnosis or MRI characteristic).

At the time of writing, we couldn't find an answer to this question (is the MRI reliable in diagnosing human lacrimal gland tumors?) in the scientific literature, even though a similar study of 39 patients exists, where patients with primary lacrimal fossa lesions were diagnosed by means of CT and had their clinical histories reviewed (Frederick A. Jakobiec, Yeo, Trokel, Abbott, Anderson, Citrin, & Alper, 1982). Similar studies for other pathologies exist (Kepple, Layeeque, Klimberg, Harms, Siegel, Korourian, Gusmano, & Henry-Tillman, 2005; Luryi, Michaelides, Babu, Bojrab, Kveton, Hong, Zappia, Sargent, & Schutt, 2019; Tse, Chaiwun, Wong, Yeung, Pang, Tang, & Cheung, 2006; Yildirim, Saatli, Kose, Sancar, Ulukus, Koyuncuoglu, Saygili, & Obuz, 2018).

Additionally, we hope to find meaningful relationships between clinical signs/symptoms or imagiological signs and the several pathological entities. Contingently on identifying some, we will try to build a regression model in order to uncover predictors of a correct image-based diagnosis. Equipped with an MRI report with those same features, the practicing doctor can then proceed safely with an appropriate therapy, with an even higher degree of confidence.

Finally, we will strive to provide a rough estimation of the incidence rate of lacrimal gland tumors in Berlin between 2011-2018 and compare it with some other studies, like von Holstein's epidemiological study for lacrimal gland lesions, the largest to date, which took place in Denmark in 2013 with data from 1974 to 2007 (Waleed M. Hassan, Mohamed S. Bakry, Housam M. Hassan, & Ahmad S. Alfaar, 2016; J. A. Shields, Bakewell, Augsburger, & Flanagan, 1984; Sarah Linéa von Holstein, Therkildsen, Prause, Stenman, Siersma, & Heegaard, 2013).

2 – Materials and Methods

2.1 Materials

2.1.1 Patients

2.1.1.1 Inclusion criteria

This retrospective unicentric case series is based on anonymized information from patients who were examined at the Charité Universitätsmedizin Berlin – Campus Benjamin Franklin and Campus Virchow-Klinikum – from 1997 to 2019. These patients were found by screening for orbital tumors and surgeries on the SAP clinical software system, according to the tenth revision of the International Statistical Classification of Diseases and Related Health Problems (ICD) of the World Health Organization (WHO) and the German procedure classification, or “Operationen- und Prozedurenschlüssel” (OPS), a German adaptation of the International Classification of Procedures in Medicine (ICPM), as well as by manual search. The ICD-10 and OPS codes used were comprehensive in order to correct for unspecific and faulty coding. They are detailed in Tables 6 and 7, respectively:

Table 6. ICD-10 codes

Code	Diagnosis
C69	Malignant neoplasm of eye and adnexa
C69.5	Lacrimal gland and duct
C69.6	Orbit
C69.8	Overlapping lesion of eye and adnexa
C69.9	Eye, unspecified
D09	Carcinoma in situ of other and unspecified sites
D09.2	Eye
D31	Benign neoplasm of eye and adnexa
D31.5	Lacrimal gland and duct
D31.6	Orbit, unspecified

D31.9	Eye, unspecified
H04	Disorders of lacrimal system
H04.0	Dacryoadenitis
H04.1	Other disorders of lacrimal gland
H04.3	Acute and unspecified inflammation of lacrimal passages
H04.4	Chronic inflammation of lacrimal passages
H04.6	Other changes in lacrimal passages
H04.8	Other disorders of lacrimal system
H04.9	Disorder of lacrimal system, unspecified

Table 7. OPS codes

Code	Diagnosis
1-52	Biopsy of eyeball through incision
1-522	Biopsy of the lacrimal gland and lacrimal passages
5-08	Surgeries of the lacrimal system
5-080	Incision of the lacrimal gland
5-080.0	… without further procedures
5-080.2	… with drainage
5-080.x	Other
5-080.y	Unspecified
5-081	Excision of lesion of lacrimal gland
5-081.0	Partial excision
5-081.1	Total excision
5-081.x	Other
5-081.y	Unspecified
5-082	Other surgeries of the lacrimal gland
5-082.0	Re-attachment
5-082.x	Other
5-082.y	Unspecified

The time period selected (from May 1997 to December 2019) was the maximum permitted by the clinical software and/or legal requirements for information safekeeping which was simultaneously compatible with a relevant search.

Patients were, then, included, if an image-based pre-operative diagnosis and a histopathological post-operative diagnosis could be found. Only patients with a clear pre-operative image-based diagnosis (e.g.: “primarily” dacryops or “main suspicion diagnosis”) were included.

2.1.1.2 Exclusion criteria

Patients whose medical history was insufficient or who did not undergo surgery were excluded immediately. Furthermore, patients whose pre-operative orbital MRI and/or histopathology report couldn’t be collected were also excluded on a second analysis.

All image-based diagnosis which were inconclusive (e.g.: lymphoma DD pleomorphic adenoma DD dacryops DD pleomorphic adenocarcinoma DD metastase) or even inexplicit (e.g.: “tumor of unclear dignity”) were excluded on a third review.

2.2 Methods

2.2.1 Clinical data

Every patient included in this thesis consented to have their clinical data used for scientific research/clinical studies. The written consent could be found in each patient's medical file, which was signed on admission to the Charité Universitätsmedizin Berlin – Campus Benjamin Franklin and Campus Virchow-Klinikum.

An initial list was created of 1,892 patients found through the ICD-10 and OPS codes. This list included the patient's name, number and date of birth, as well as the corresponding ICD-10 code and file number. The virtual medical files from this initial list were then perused utilizing the SAP clinical software system.

In cases where the histopathological report confirmed a lacrimal gland lesion, the relevant medical files, when available, were individually requested from the hospital's central archive. This was done by filling out a paper form with the patient's full name and date of birth, as well as the destination to have the files delivered. Each form required a hand signature. Therefore, a secondary list was created.

The medical information of 208 patients (secondary list), with several files per patient, was mostly requested from 1/2016 to 12/2018. Some files were also requested from 1/2019 to 12/2019. This was done, however, using PEGASUS archive software, which came to replace the paper form system. Consequently, from then on, it was not necessary to input patients' data explicitly.

From the secondary list, patients were selected where a clear image-based pre-operative diagnosis and a histopathological post-operative diagnosis could be found, creating a final list. The final list, encompassing 112 patients, represents the basis of the work presented on this thesis.

Additional clinical data was also collected from the patients of the final list. This data was comprised of:

1. Patient Identification Data:
   Full name, date of birth, gender (female or male).

2. Pre-Operative Clinical Data:
   Date of first visit; laterality (unilateral or bilateral); affected eye (right or left), visual acuity (in decimal values) and eye pressure (mmHg) on the first visit; time from first complaint to first visit; presence of pain, proptosis, ptosis, swelling and diplopia; date of first MRI.
3. MRI-associated data:
   Size of lesion, margins of lesion, presence of bone erosion, signs of perineural invasion, contrast agent used, strength of the magnetic field, surface coil used, internal features (T1- and T2-weighted images), degree of contrast enhancement, and use of DWI/DCE sequences.
4. Therapy:
   Excisional biopsy, incisional biopsy, enucleation, chemotherapy, radiotherapy, systemic corticosteroid, or any combination of these.
5. Surgery:
   Surgery performed and date of surgery.
6. Follow-up:
   Visual acuity and eye pressure on the first follow-up after surgery; date of last visit; recurrence and date of recurrence.

The primary outcome measure was the degree of correspondence between the pre-operative orbital MRI diagnosis and the histopathologic findings.

The secondary outcome measures included the development of predictive models for the correct diagnosis of lacrimal tumors through MRI, as well as measuring associations between any two variables of interest.

Lastly, a detailed analysis of the demographics and lesion data of the patients' cohort was performed.

2.2.2 Statistics

Sample proportion tests were conducted to describe the clinical data.

The interdependence of the symptoms/signs and the pathological diagnosis was assessed with a Chi-square test with a Monte Carlo estimate for the exact test with a

1% level of significance (in 1 million samples) and Bonferroni correction, since the data violated the Chi-square test assumptions of asymptotic significance (Cohen, 1969). The same study was employed for the MRI findings. A Cramer's V test helped determine the strength of the associations, with the results being interpreted as follows: < 0.05 was seen as a weak or very weak association; between 0.05 and 0.15 as a moderate association; > 0.15 to 0.25 as strong; and > 0.25 as very strong (Akoglu, 2018). The likelihood ratio with asymptotic significance was also calculated.

The Cohen's kappa test was used to determine the degree of agreement between the MRI diagnosis and the pathologic diagnosis (overall and in a selected number of groups of patients), with Cohen's kappa coefficient (k) measure of agreement being interpreted as follows: <0.2 poor; 0.21-0.4 fair; 0.41-0.6 moderate; 0.61-0.8 good; and 0.81-1.0 very good (Sun, 2011).

Basic measures of diagnostic accuracy were employed, namely sensitivity, specificity, positive predictive value (PPV), and negative predictive value (NPV) (Šimundić, 2009).

A crude incidence rate for lacrimal gland tumors which were presented at our hospital between 2011 and 2018 in the region of Berlin, as well as a gender- and age-specific incidence rate, was calculated. Gender was divided into male and female, whereas age was divided into 8 groups (0 to 20 years, 21-30, 31-40, 41-50, 51-60, 61-70, 71-80 and greater than 80). The data regarding Berlin's population was obtained from the Federal Statistical Office of Germany (https://www-genesis.destatis.de) from the last census (2011) performed before the last year of data available (2018). We settled on this time period, since the records of patients in from our hospital is greatly scarcer prior to 2010, which can be explained by the deletion of outpatient files from the archive after 10 years. The rates were expressed in cases per 1 million person-years and the 95% confidence intervals were calculated by assuming a Poisson distribution. An incidence rate ratio between males and females was also calculated (Frome, 1983; Xu, Cheung, Lam, Tan, & Milligan, 2010).

In order to ascertain the predictive capability of various models in identifying a correct MRI diagnosis (after comparison with the histopathological diagnosis) based on some variables from our collected data, logistic regressions using the enter method were performed. Patients with an unclear/unspecified or irrelevant MRI diagnosis were

excluded. Simultaneously, a Hosmer-Lemeshow Test was performed to rule out eventual misspecifications in the model (Menard, 2011). To compare the importance of the different variables in our model, a standardized beta weight was calculated, utilizing the mean predicted probability, standard deviation of the variable and unstandardized beta weight of the logit of the same variable (King, 2007). Afterwards, the same set of studies were conducted on subgroups corresponding to each pathologic diagnosis.

Statistical analysis was performed using SPSS (Version 25, IBM, New York, USA) and statistical significance was defined as $p < 0.05$ or smaller, when taking the Bonferroni correction into account.

2.2.3 Ethics

The study adhered to the tenets of the Declaration of Helsinki.

3 - Results

Overall, 112 patients were included. Of these, 73 (65.2%) were female, with this predilection being statistically significant (p-value < 0.001). The mean age with standard deviation, median age, and age range were 53.29 ± 18.01, 55, and 2-92 years old, respectively.

The mean best-corrected visual acuity (BCVA) was 0.82 ± 0.23 decimal (pertaining to 103 patients) and the mean intra-ocular pressure (IOP) measured (from 68 patients) was 17.5 ± 4.3 mmHg.

The results of the pathology examinations are presented in Table 8, along with the corresponding demographic data of the patients, showing that dacryoadenitis was the most common diagnosis (~40%), followed by lymphoma (~19%) and pleomorphic adenoma (~12%).

Table 8. Patient demographics

Pathologic diagnosis	*n* (%)	Gender (M/F)	Mean Age (years old) ± Std. Deviation	Median Age, (Range)
Dacryoadenitis	45 (40.2%)	12/33	51.73 ± 17.45	54, (2-78)
Lymphoma	21 (18.8%)	6/15	62.43 ± 14.12	64, (35-92)
Pleomorphic adenoma	13 (11.6%)	7/6	49.15 ± 17.78	48, (24-78)
BRLH	10 (8.9%)	3/7	44.4 ± 14.29	39, (27-70)
Adenoid cystic carcinoma	7 (6.3%)	2/5	61.43 ± 22.31	64, (29-89)
Dacryops	6 (5.4%)	3/3	60.17 ± 15.36	58, (42-87)
Pleomorphic adenocarcinoma	5 (4.5%)	3/2	61.20 ± 16.35	59, (39-84)
Cavernous hemangioma	2 (1.8%)	1/1	5 and 35	-
Cystic Teratoma	1 (0.9%)	1/0	23	-
Chalazion	1 (0.9%)	0/1	46	-
Solitary Fibrous Tumor	1 (0.9%)	1/0	40	-
X^2	*168.1*	*10.3*	*39.7*	
p-value	***<0.001***	***<0.001***	*0.968*	-
Total	112	39/73	53.29 ± 18.01	55, (2-92)

RESULTS

The overall crude incidence rate for patients from the Berlin region with a viable histopathological diagnosis for a lacrimal gland tumor, who came to our hospital between 2011 and 2018, was 1.93/1,000,000/year [95% CI: 1.67 – 2.2].

The incidence rate calculations for the several age groups and genders are shown in Table 9.

Table 9. Incidence rate of biopsied lacrimal gland tumors at the Charité Berlin between 2011 and 2018

	Lesions (n)	Incidence per 1,000,000 [95% CI]
Age		
0-20	1	0.20 [0 - 0.39]
21-30	5	1.20 [0.66 - 1.74]
31-40	6	1.42 [0.84 - 2.01]
41-50	12	3.00 [2.13 - 3.86]
51-60	11	2.89 [2.02 - 3.76]
61-70	13	4.48 [3.24 - 5.73]
71-80	4	1.55 [0.78 - 2.33]
>81	2	1.76 [0.51 - 3.00]
Gender		
Male	20	1.46 [1.14 - 1.79]
Female	34	2.38 [1.97 - 2.79]

We can observe that the age group with the highest incidence rate was the one with patients between 61 and 70 years old (4.48; 95% CI: 3.24 – 5.73), whereas the lowest incidence rate was observed in patients under 20 years old (0.20; 95% CI: 0 – 0.39), with this difference being statistically significant.

The incidence rate ratio between females and males was 1.63 [95% CI: 1.23 – 2.16].

These lesions were equally distributed between the left and right side and only eight patients showed a bilateral occurrence, with that representing 11% (*n* = 5) of all cases of dacryoadenitis and 14% (*n* = 3) of all cases of lymphoma (Table 10). The remaining groups of lacrimal lesions were unilateral in all patients. The mean time to diagnosis showed a great dispersion, this result being greatest in pleomorphic adenoma (494

days) and lowest in pleomorphic adenocarcinoma (161 days). The average time to diagnosis of all patients was 287 days with a standard deviation of 469 days.

Table 10. Patients' pre-operative clinical data

Pathologic diagnosis	R/L (*n*)	OU	Mean BCVA (dec)	IOP (mmHg)	Mean Time to Diagnosis (days)
Dacryoadenitis	18/22	5 (11.1%)	0.85 ± 0.2	17.8 ± 5.2	218.5 ± 549.7
Lymphoma	7/11	3 (14.3%)	0.78 ± 0.24	17.3 ± 4.0	170.4 ± 133.6
Pleomorphic adenoma	11/2	-	0.92 ± 0.11	17.1 ± 3.6	493.8 ± 428.9
BRLH	3/7	-	0.9 ± 0.16	15.3 ± 4.6	405 ± 427
Adenoid cystic carcinoma	3/4	-	0.54 ± 0.46	19.7 ± 2.9	384 ± 595.3
Dacryops	4/2	-	0.83 ± 0.19	19.3 ± 2.1	273.3 ± 243.8
Pleomorphic adenocarcinoma	3/2	-	0.63 ± 0.47	15 ± 0	161.3 ± 145.6
Total	51/53	8 (7.1%)	0.82 ± 0.23	17.5 ± 4.3	286.5 ± 468.5

R = right eye; L = Left eye; OU = both eyes

The proportion of epithelial (*n* = 31) lacrimal lesions, when excluding non-lacrimal lesions, was thus 28.7%. From these, 61% (*n* = 19) were benign. Adenoid cystic carcinoma (*n* = 7) was the most common PEMLG, followed by pleomorphic adenocarcinoma (*n* = 5).

Dacryoadenitis amounted to 59% of all non-epithelial lesions and lymphoma to 27.6%.

From the 45 cases of dacryoadenitis, 4 (8.9%) were associated with sarcoidosis and a further 4 (8.9%) with IgG4-related disease. The remaining 37 (82.8%) were shown to be idiopathic. Concerning the 21 cases of lymphoma, 10 (47.6%) were extranodal marginal zone lymphomas, this being the most frequent subtype of all. The remaining cases and their corresponding subtype are represented in Table 11.

RESULTS

Table 11. Observed cases of lymphoma

Extranodal marginal zone lymphoma	10/21 (47.6%)
Diffuse large B-cell-lymphoma	4/21 (19.0%)
Mantle cell lymphoma	4/21 (19.0%)
Follicular lymphoma	3/21 (14.3%)

In Table 12 it is showed how the image-based diagnosis of 107 patients compared to the post-operative histopathologic diagnosis. Ignoring the cases with just one patient per diagnosis, we could observe that, dacryops (with 83%), followed by dacryoadenitis, (with 73%), were the MRI diagnosis with the greatest hit ratio to the pathologic diagnosis. Lymphoma, pleomorphic adenoma and the PEMLG all achieved an agreement of around 50%. Meningeoma, lymphoepithelioma and neurofibroma were MRI-based diagnosis, which were not contemplated in any histopathologic counterpart. In return, some histopathologic diagnosis, such as chalazion, solitary fibrous tumor, and cystic teratoma didn't correspond to any MRI-diagnosis, and so, their results were aggregated under "Other" [diagnosis].

Table 12. Crosstabulation of pre-operative orbital MRI diagnosis and corresponding histopathologic diagnosis

MRI Diagnosis	***Histopathologic diagnosis***								
	Dacryoadenitis	Dacryops	Pleomorphic Adenoma	Ad. Cy. Carcinoma or Pleo. Carcinoma	Lymphoma	Cavernous Hemangioma	BRLH	Other	TOTAL
Dacryoadenitis	24 (72.7%)	1 (3%)	1 (3%)	-	5 (15%)	0	2 (6%)	0	33 (30.8%)
Dacryops	-	5 (83.3 %)	-	-	-	-	1 (16.7 %)	-	6 (5.6%)
Pleomorphic adenoma	6 (35.3%)	-	8 (47%)	-	-	1 (6%)	2 (11.8%)	-	17 (15.9%)
Adenoid cystic carcinoma or Pleomorphic carcinoma	2 (12.5%)	-	2 (12.5%)	8 (50%)	-	-	2 (12.5%)	2 (12.5%)	16 (15%)
Lymphoma	10 (33.3%)	-	-	3 (10%)	15 (50%)	-	1 (3.3%)	1 (3.3%)	30 (28%)
Meningeoma	1 (100%)	-	-	-	-	-	-	-	1 (0.9%)
Cavernous Hemangioma	-	-	-	1 (100%)	-	-	-	-	1 (0.9%)
Lymphoepithelioma	-	-	-	-	1 (100%)	-	-	-	1 (0.9%)
BRLH	-	-	-	-	-	-	1 (100%)	-	1 (0.9%)
Neurofibroma	-	-	1 (100%)	-	-	-	-	-	1 (0.9%)
TOTAL	43 (40.2%)	6 (5.6%)	12 (11.2%)	12 (11.2%)	21 (19.6%)	1 (0.9%)	9 (8.4%)	3 (2.8%)	107

Other corresponds to "Other diagnosis", which aren't listed, such as: Chalazion, solitary fibrous tumor and cystic teratoma

RESULTS

The overall degree of correspondence between the pre-operative orbital MRI diagnosis and the histopathologic findings was ascertained, revealing a moderate agreement of k=0.451 and p-value <0.001, as can be observed in Table 13 (Sun, 2011).

Table 13. Degree of correspondence between pre-operative orbital MRI diagnosis and corresponding histopathologic diagnosis

Cohen's kappa test MRI/histopathologic diagnosis				
Measure of agreement	# cases	Value	Confidence Interval	p-value
Kappa	107	0.451	[0.335-0.567]	<0.001

The measures of test accuracy for the major pre-operative MRI diagnoses can be found in Table 14. We can observe that dacryoadenitis was the diagnosis with the lowest sensitivity (at 57%) and NPV (at 61%). Dacryops showed the highest parameters of sensitivity, specificity, PPV and NPV, with them being 83%, 99%, 83%, and 94%, respectively. Lymphoma, pleomorphic adenoma and PEMLG achieved similar results (Šimundić, 2009).

Table 14. Measures of accuracy for major pre-operative MRI diagnoses

MRI diagnosis	**Sensitivity**	**Specificity**	**PPV**	**NPV**
Dacryoadenitis	0.57	0.86	0.73	0.61
Dacryops	0.83	0.99	0.83	0.94
Pleomorphic adenoma	0.73	0.91	0.47	0.90
Adenoid cystic carcinoma or Pleomorphic carcinoma	0.73	0.92	0.50	0.90
Lymphoma	0.75	0.83	0.50	0.81

PPV, positive predictive value; NPV, negative predictive value

RESULTS

Patients' symptoms and signs observed during the clinical history and examination are outlined in Table 15, along with the results of the Chi-square tests and their statistical significance. Overall, we can perceive that there is a statistically significant interdependence between proptosis/swelling and pathologic diagnosis. The Cramer's V for both associations was also statistically significant (p-values of 0.001 and 0.002, respectively), with a value of 0.451 corresponding to a very strong association (Akoglu, 2018).

Table 15. Patients' symptoms and signs

Pathologic diagnosis	**Pain** *n*/Total (%)	**Proptosis** *n*/Total (%)	**Ptosis** *n*/Total (%)	**Swelling** *n*/Total (%)	**Diplopia** *n*/Total (%)
Dacryoadenitis	4/44 (9.1%)	11/44 (25%)	13/44 (29.5%)	41/45 (91.1%)	6/44 (13.6%)
Lymphoma	1/21 (4.8%)	4/21 (19%)	8/21 (38.1%)	17/21 (81%)	3/21 (14.3%)
Pleomorphic adenoma	1/13 (7.7%)	8/13 (61.5%)	1/13 (7.7%)	6/12 (50%)	2/13 (15.4%)
BRLH	0/10 (0%)	2/10 (20%)	1/10 (10%)	4/10 (40%)	1/10 (10%)
Adenoid cystic carcinoma	1/7 (14.3%)	6/7 (85.7%)	2/7 (28.6%)	4/7 (57.1%)	3/7 (42.9%)
Dacryops	0/6 (0%)	0/6 (0%)	0/6 (0%)	6/6 (100%)	0/6 (0%)
Pleomorphic adenocarcinoma	2/4 (50%)	2/4 (50%)	2/4 (50%)	3/4 (75%)	2/4 (50%)
X^2	*10.969*	*21.374*	*8.868*	*21.366*	*8.754*
p-value	*0.093*	***0.001***	*0.176*	***0.002***	*0.171*
[99% Conf. Interval]	*[0.092-0.094]*	*[0.001-0.001]*	*[0.175-0.177]*	*[0.002-0.002]*	*[0.170-0.172]*
Cramer's V	*0.323*	*0.451*	*0.291*	*0.451*	*0.289*
Total	9/110 (8.2%)	35/110 (31.8%)	30/110 (27.3%)	81/110 (73.6%)	18/110 (16.4%)

RESULTS

The chief complaint from 81 (73.6%) patients was swelling of the temporal region of the upper eyelid. The symptom least mentioned was pain, with only 9 (8.2%) patients stating it, and with no reports from patients with dacryops or benign reactive lymphoid hyperplasia.

One (14.3%) and two (50%) patients with adenoid cystic carcinoma and pleomorphic adenocarcinoma, respectively, complained of pain, which was shown to have a statistically significant relationship to pleomorphic adenocarcinoma (p-value = 0.0025; p-value with Bonferroni correction = 0.00357; see Table 16). Diplopia was also disproportionally present in these two groups, with rates as high as 42.9% and 50%, respectively.

A statistically significant dependence was also found between proptosis and adenoid cystic carcinoma (Table 17), swelling and dacryoadenitis, and swelling and BRLH (Table 18). Ptosis and diplopia did not show a statistically significant association with any of the histopathologic diagnoses (Tables 19 and 20).

Table 16. Crosstabulation of histopathologic diagnosis and pain as a symptom

Pathologic diagnosis	**Pain *n* (%)**							
	No		Yes		*p-value*	TOTAL
Dacryoadenitis	40	(90.9%)	4	(9.1%)	*0.8717*	44
Dacryops	6	(100%)	0	(0%)	*0.4399*	6
Pleomorphic adenoma	12	(92.3%)	1	(7.7%)	*0.9037*	13
Adenoid cystic carcinoma	6	(85.7%)	1	(14.3%)	*0.5762*	7
Lymphoma	20	(95.2%)	1	(4.8%)	*0.4857*	21
BRLH	10	(100%)	0	(0%)	*0.3087*	10
Pleomorphic adenocarcinoma	2	(50%)	2	(50%)	***0.0025***	4
TOTAL	96 (91%)		9 (9%)		-	105

Likelihood Ratio of 8.24 with p-value = 0.221;
P-value with Bonferroni correction = 0.00357

Table 17. Crosstabulation of histopathologic diagnosis and proptosis as a symptom

Pathologic diagnosis	Proptosis *n* (%)						*p-value*	TOTAL
	No			Yes				
Dacryoadenitis	33	(75%)		11	(25%)		*0.2282*	44
Dacryops	6	(100%)		0	(0%)		*0.0877*	6
Pleomorphic adenoma	5	(38.5%)		8	(61.5%)		*0.0125*	13
Adenoid cystic carcinoma	1	(14.3%)		6	(85.7%)		***0.0014***	7
Lymphoma	17	(81%)		4	(19%)		*0.1718*	21
BRLH	8	(80%)		2	(20%)		*0.4131*	10
Pleomorphic adenocarcinoma	2	(50%)		2	(50%)		*0.4146*	4
TOTAL	72	(68.6%)		33	(31.4%)		-	105

Cramer's V = 0.451, p-value < 0.001;
Likelihood Ratio of 22.17 with p-value = 0.001
P-value with Bonferroni correction = 0.00357

Table 18. Crosstabulation of histopathologic diagnosis and swelling as a symptom

Pathologic diagnosis	Swelling *n* (%)						*p-value*	TOTAL
	No			Yes				
Dacryoadenitis	4	(8.9%)		41	(91.1%)		***0.0032***	45
Dacryops	0	(0%)		6	(100%)		*0.1697*	6
Pleomorphic adenoma	6	(50%)		6	(50%)		*0.0173*	12
Adenoid cystic carcinoma	3	(42.9%)		4	(57.1%)		*0.1921*	7
Lymphoma	4	(19%)		17	(81%)		*0.6421*	21
BRLH	6	(60%)		4	(40%)		***0.0033***	10
Pleomorphic adenocarcinoma	1	(25%)		3	(75%)		*0.9171*	4
TOTAL	24	(22.9%)		81	(77.1%)		-	105

Cramer's V = 0.451 with p-value = 0.002;
Likelihood Ratio of 21.28 with p-value = 0.002
P-value with Bonferroni correction = 0.00357

Table 19. Crosstabulation of histopathologic diagnosis and ptosis as a symptom

Pathologic diagnosis	Ptosis *n* (%)					
	No		Yes		*p-value*	TOTAL
Dacryoadenitis	31	(70.5%)	13	(29.5%)	*0.4455*	44
Dacryops	6	(100%)	0	(0%)	*0.1378*	6
Pleomorphic adenoma	12	(92.3%)	1	(7.7%)	*0.1122*	13
Adenoid cystic carcinoma	5	(71.4%)	2	(28.6%)	*0.8579*	7
Lymphoma	13	(61.9%)	8	(38.1%)	*0.1467*	21
BRLH	9	(90%)	1	(10%)	*0.2320*	10
Pleomorphic adenocarcinoma	2	(50%)	2	(50%)	*0.2572*	4
TOTAL	78 (74.3%)		27 (25.7%)		-	105

Likelihood Ratio of 10.91 with p-value = 0.091

P-value with Bonferroni correction = 0.00357

Table 20. Crosstabulation of histopathologic diagnosis and diplopia as a symptom

Pathologic diagnosis	Diplopia *n* (%)					
	No		Yes		*p-value*	TOTAL
Dacryoadenitis	38	(70.5%)	6	(29.5%)	*0.5462*	44
Dacryops	6	(100%)	0	(0%)	*0.2675*	6
Pleomorphic adenoma	11	(92.3%)	2	(7.7%)	*0.9328*	13
Adenoid cystic carcinoma	4	(71.4%)	3	(28.6%)	*0.0474*	7
Lymphoma	18	(61.9%)	3	(38.1%)	*0.7911*	21
BRLH	9	(90%)	1	(10%)	*0.5764*	10
Pleomorphic adenocarcinoma	2	(50%)	2	(50%)	*0.0613*	4
TOTAL	88 (83.8%)		17 (16.2%)		-	105

Likelihood Ratio of 7.95 with p-value = 0.24;

P-value with Bonferroni correction = 0.00357

RESULTS

A logistic regression between a correct MRI diagnosis and the aforementioned five clinical signs and symptoms showed statistical significance for “Swelling” (p-value = 0.031), as can be seen in Table 21, with pain (p-value = 0.335) being the second factor most close to it. Furthermore, the Hosmer-Lemeshow Test for our model was not statistically significant (p-value of 0.755).

The model was based on the clinical data of 100 patients and showed an improved predictive capacity for a correct MRI diagnosis, with 64.0% of cases being correctly predicted, as compared to the base model (without the five clinical signs), where only 60.0% of cases were correctly predicted. The Nagelkerke R^2 of the model was 9.0%. However, as a whole, this increased predictive capacity was not shown to be statistically significant, since its p-value was 0.23.

Table 21. Logistic Regression Model: Correct MRI Diagnosis*Clinical signs and symptoms

Base model

Observed CDx[1]	Predicted CDx	
	No	Yes
No	0	40
Yes	0	60

Overall % Correct	60%

Model with Data from clinical signs and symptoms

Observed CDx[1]	Predicted CDx	
	No	Yes
No	12	28
Yes	8	52

Overall % Correct	64%

[1]CDx stands for “correct diagnosis”

Model summary

-2 Log likelihood	Cox & Snell R Square	Nagelkerke R Square
127.748	0.066	0.09

p-value = 0.23

Hosmer-Lemeshow Test		
Chi-square	df	Significance
2.643	5	0.755

Variables in the model

	B	S.E.	Wald	df	p-value	Exp(B)	BwX[2]
Pain	0.833	0.864	0.931	1	0.335	2.301	0.057
Proptosis	0.208	0.531	0.154	1	0.695	1.231	0.024
Ptosis	0.069	0.500	0.019	1	0.889	1.072	0.007
Swelling	1.101	0.509	4.671	1	**0.031**	3.007	0.116
Diplopia	0.425	0.692	0.377	1	0.539	1.530	0.038

[2]BwX stands for Standardized Beta Weight for X

The standardized beta weight for swelling was 0.116 with an odds ratio of 3.007 [1.108 – 8.160], while for pain it was 0.057 and 2.301 [0.423 – 12.502], with these two variables again being the most relevant ones in the model.

Logistic regression models were also attempted on subgroups organized by diagnosis. However, in all cases the sample size was too small and/or no statistically significant variable could be found.

The MRI findings which were able to be collected from the MRI reports of different origins and disparate detail are outlined in Table 22, along with the results of the Chi-square tests and their statistical significance. The associations found between the MRI findings and the pathologic diagnosis are represented in Tables 23 to 25. Overall, we can see a statistically significant interdependence between all MRI findings and pathologic diagnosis. The Cramer's V for the associations was very strong and also statistically significant, showing a value of 0.54 (p-value = 0.001) for bone erosion, of 0.44 (p-value = 0.03) for the margins of the lesion, and of 0.7 (p-value of 0.001) for perineural invasion (Akoglu, 2018).

RESULTS

Table 22. MRI findings

Pathologic diagnosis	Bone Erosion	Regular Margins	Neural Invasion
Dacryoadenitis	0/40 (0%)	20/30 (66.7%)	0/40 (0%)
Lymphoma	0/20 (0%)	5/14 (35.7%)	0/20 (0%)
Pleomorphic adenoma	2/12 (16.7%)	9/9 (100%)	0/10 (0%)
BRLH	1/10 (10%)	3/4 (75%)	0/10 (0%)
Adenoid cystic carcinoma	3/5 (60%)	3/5 (60%)	0/7 (0%)
Dacryops	1/6 (16.7%)	3/3 (100%)	0/6 (0%)
Pleomorphic adenocarcinoma	2/5 (40%)	1/3 (33.3%)	2/4 (50%)
X^2	*28.458*	*13.276*	*47.479*
p-value	***0.001***	***0.03***	***0.001***
[99% Conf. Interval]	*[0.001-0.001]*	*[0.029-0.03]*	*[0.001-0.001]*
Cramer's V	*0.539*	*0.442*	*0.7*
Total	9/98 (9.2%)	44/68 (64.7%)	2/97 (2.1%)

The most common configuration of a typical lacrimal gland tumor on MRI was shown to be grossly a well-circumscribed tumor with a mean of 22.53 mm as its greatest dimension (Fig. 9), without perineural invasion and without bone erosion.

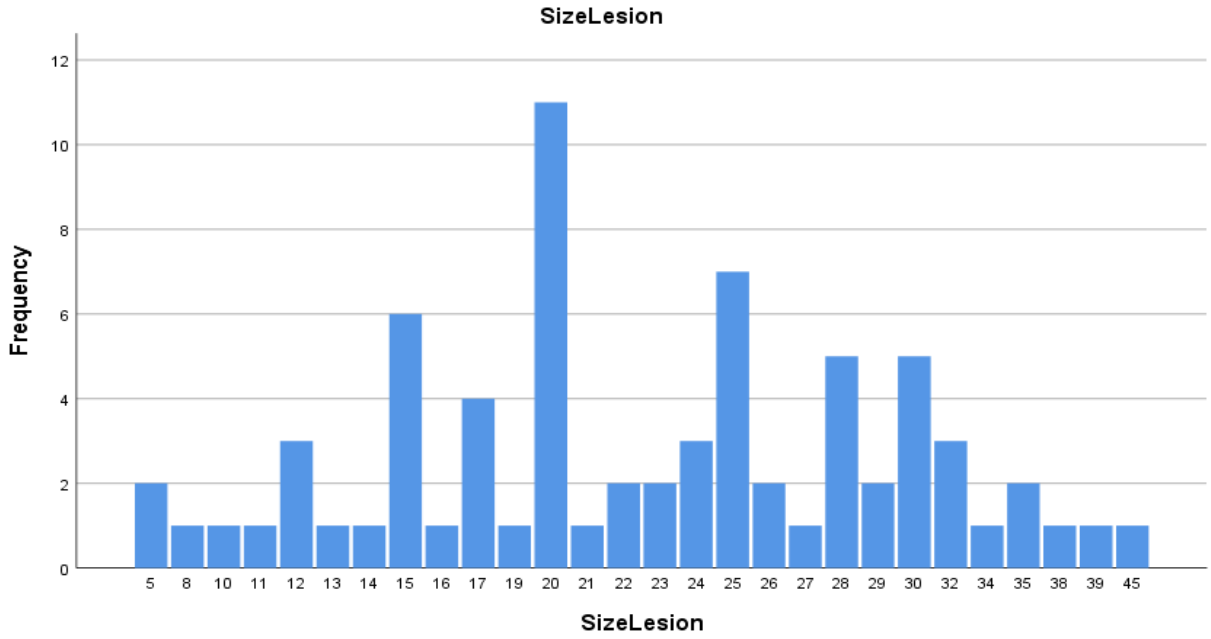

Fig. 9: Distribution of the greatest dimension of lacrimal gland tumors from 72 patients' MRI reports

RESULTS

The median value of the greatest dimension was 22.5 mm, with minimum and maximum values of 5 mm and 45 mm, respectively. The standard deviation was 7.993 mm. This broad description also represents the usual configuration of the benign lacrimal gland tumors observed in Table 22.

The typical configuration of a PEMLG, based on 8 reported cases (5 with adenoid cystic carcinoma and 3 with pleomorphic adenocarcinoma), was, in comparison to the typical benign lacrimal gland tumor, more likely to be bigger, cause bone erosion, have irregular margins and exhibit perineural invasion. Its mean greatest dimension was 29.75 mm, with a median of 30 mm and standard deviation of 9.736 mm. The minimum and maximum values were 20 mm and 45 mm, respectively. The frequency of bone erosion was higher in PEMLG, as seen in Table 22. In fact, bone erosion was a hallmark of adenoid cystic carcinoma, with 3 (60%) of the patients' MRI examinations showing this characteristic to some extent and the relation between bone erosion and adenoid cystic carcinoma being statistically significant (p-value <0.001, see Table 23).

Table 23. Crosstabulation of histopathologic diagnosis and bone erosion in the MRI

Pathologic diagnosis	**Bone Erosion *n* (%)**							
	No		Yes		*p-value*	TOTAL
Dacryoadenitis	40	(100%)	0	(0%)	*0.0089*	40
Dacryops	5	(83.3%)	1	(16.7%)	*0.5124*	6
Pleomorphic adenoma	10	(83.3%)	2	(16.7%)	*0.3380*	12
Adenoid cystic carcinoma	2	(40%)	3	(60%)	***0.0001***	5
Lymphoma	20	(100%)	0	(0%)	*0.1109*	20
BRLH	9	(90%)	1	(10%)	*0.9248*	10
Pleomorphic adenocarcinoma	3	(60%)	2	(40%)	*0.0143*	5
TOTAL	89	(90.8%)	9	(9.2%)	-	98

Cramer's V = 0.539 with p-value < 0.001;
Likelihood Ratio of 23,94 with p-value < 0.001
P-value with Bonferroni correction = 0.00357

RESULTS

From the crosstabulation in Table 24, it's clear that perineural invasion was only detected in 2 patients with pleomorphic adenocarcinoma (from a total of 4) and that this was also a statistically significant association (p-value < 0.001).

Table 24. Crosstabulation of histopathologic diagnosis and perineural invasion in the MRI

Pathologic diagnosis	**Perineural invasion *n (%)***							
	No		Yes		*p-value*	TOTAL
Dacryoadenitis	40	(100%)	0	(0%)	*0.2313*	40
Dacryops	6	(100%)	0	(0%)	*0.7137*	6
Pleomorphic adenoma	10	(100%)	0	(0%)	*0.6280*	10
Adenoid cystic carcinoma	7	(100%)	0	(0%)	*0.6902*	7
Lymphoma	20	(100%)	0	(0%)	*0.4664*	20
BRLH	10	(100%)	0	(0%)	*0.6280*	10
Pleomorphic adenocarcinoma	2	(50%)	2	(50%)	***<0.0001***	4
TOTAL	95 (97.9%)		2 (2.1%)		-	97

Cramer's V = 0.7 with p-value < 0.001;
Likelihood Ratio of 13.94 with p-value = 0.03
P-value with Bonferroni correction = 0.00357

Regarding the lesion's margins, no statistically significant relationship to pathologic diagnosis was found. Still, it can be observed in Table 25 that lymphomas showed a higher-than-expected number of tumors with irregular margins than the typical lacrimal gland tumor (p-value of 0.0109; p-value with Bonferroni correction = 0.00357), but also neither bone erosion nor perineural invasion (Table 22).

RESULTS

Table 25. Crosstabulation of histopathologic diagnosis and margins of lesion in the MRI

Pathologic diagnosis	Margins of lesion *n* (%)							TOTAL
	Irregular		Regular		*p-value*			
Dacryoadenitis	10	(33.3%)	20	(66.7%)	*0.7637*			30
Dacryops	0	(0%)	3	(100%)	*0.1907*			3
Pleomorphic adenoma	0	(0%)	9	(100%)	*0.0174*			9
Adenoid cystic carcinoma	2	(40%)	3	(60%)	*0.8191*			5
Lymphoma	9	(64.3%)	5	(35.7%)	*0.0109*			14
BRLH	1	(25%)	3	(75%)	*0.6570*			4
Pleomorphic adenocarcinoma	2	(66.7%)	1	(33.3%)	*0.2448*			3
TOTAL	24 (35.3%)		44 (64.7%)		-			68

Cramer's V = 0.442 with p-value = 0.03;
Likelihood Ratio of 16.81 with p-value = 0.01
P-value with Bonferroni correction = 0.00357

Regarding the MRI examinations, which were mostly performed outside of our clinic, the following data could be attained: from 56 reports, the most commonly used strength of magnetic field was 1.5 T, being employed in the examination of 42 patients (75%), followed by 3 T (23% of patients) and with just one case of 1 T, as can be seen in Table 26; from 45 reports, the most frequently used contrast agent was gadoterate, being administered to 15 patients (33.3%), followed by gadobutrol and gadopentetate (both given to 10 patients or 22.2% of the total), as represented in Table 27; from 37 patients, only 13 (35.1%) underwent the MRI examination with an orbital coil, with the remaining 24 (64.9%) being examined with a head coil; from 107 patients, only 9 (8.4%) were examined utilizing DWI and DCE sequences.

Table 26. Strength of magnetic field

Strength of magnetic field	*n* (%)
1.0	1 (1.8%)
1.5	42 (75%)
3.0	13 (23.2%)
Total	56 (100%)

Table 27. Different contrast agents used

Contrast agent	*n* (%)
Gadolinium	9 (20%)
Gadoteridol	1 (2.2%)
Gadobutrol	10 (22.2%)
Gadoterate	15 (33.3%)
Gadopentetate	10 (22.2%)
Total	45 (100%)

In Table 28, we find the degree of correspondence between pre-operative orbital MRI diagnosis and corresponding histopathologic diagnosis, when taking just a certain group of patients into account, which were selected based on the beforementioned specifications of the MRI examination (magnetic field strength, contrast agent, coil used and DWI sequences).

Regarding the magnetic field strength, one can observe that the 3T examination (k=0.458) achieved a higher degree of agreement than the 1.5T (k=0.345) and also higher than the overall result (k=0.451). These results were statistically significant. However, the same can not be said when comparing them to each other, as can be observed through the confidence intervals in Table 28 (Sheskin, 2004).

In case of the different contrast agents used, all sub-groups showed an inferior degree of agreement than the overall result, with just the sub-group Gadobutrol not achieving statistically significance in itself.

Table 28. Degree of correspondence between pre-operative orbital MRI diagnosis and corresponding histopathologic diagnosis from the different groups of patients

Cohen's kappa test MRI/histopathologic diagnosis (subgroups)				
Group of patients	# cases	Value	Confidence Interval	p-value
1.5 T	42	0.345	0.178 - 0.512	**0.001**
3 T	13	0.458	0.137 - 0.779	**0.004**
Gadolinium	9	0.390	0.112 - 0.668	**0.005**
Gadobutrol	10	0.265	0.000 - 0.559	0.072
Gadoterate	15	0.364	0.052 - 0.676	**0.008**
Gadopentetate	10	0.405	0.103 - 0.707	**0.001**
Orbital coil	13	0.107	0.000 - 0.405	0.409
Head coil	24	0.444	0.211 - 0.677	**<0.001**
DWI	9	0.118	0.000 - 0.308	0.423

In respect to the coils used, the sub-group Head coil showed a moderate degree of correspondence (k=0.444, p-value <0.001), while the result for the sub-group Orbital coil was not statistically significant.

Lastly, the result for the group of patients who underwent DWI sequences showed a poor degree of agreement (k=0.118) and was also not statistically significant (p-value equal to 0.423).

A logistic regression model based on these four groups was also attempted. However, as represented in Table 29, no group/variable could account for a statistically significant improvement of the predictive capacity of the model. The variable which came closest to it was the “magnetic field” one, achieving a p-value of 0.218 with an Odds ratio of 2.379.

Table 29. Variables and their contributions to a logistic Regression Model: Correct MRI Diagnosis*MRI specifications

Variables in the model

	B	S.E.	Wald	df	p-value	Exp(B)
Contrast agent	0.462	0.455	1.029	1	0.310	1.587
Magnetic field	0.867	0.703	1.518	1	0.218	2.379
Coil	0.773	0.962	0.645	1	0.422	2.165
DWI	-0.510	1.120	0.207	1	0.649	0.601

The internal features of the MRI examinations and degree of contrast enhancement, as well as their relationships with the pathologic diagnosis were studied and are portrayed in Tables 30 to 32.

Overall, we can observe that there is a statistically significant interdependence between contrast agent enhancement and pathologic diagnosis ($X^2 = 38.6$; p-value < 0.001). The Cramer's V for this association was also statistically significant (p-value < 0.001), with a value of 0.58 corresponding to a very strong association (Akoglu, 2018).

Starting with the non-epithelial tumors, we can note that dacryoadenitis did not show constant internal features in T1- and T2-weighting, but contrast enhancement was rarely not observed. On the other hand, lymphomas were mainly hypointense in T1 and isointense in T2, with a moderate degree of contrast enhancement. As expressed in Table 31, the relationship between lymphoma and isointense internal features in the T2-weighted image was statistically significant (p-value of 0.0025; p-value with Bonferroni correction = 0.00278).

In regards to PEMLG, the adenoid cystic carcinoma was shown to be hypointense in T1-weighted imaging, somewhat more hypointense than hyperintense in T2 and to have a moderate to high contrast enhancement. The pleomorphic adenoma resembled these same characteristics, differing in the T2-weighted imaging, where it was chiefly hyperintense.

RESULTS

Table 30. Crosstabulation of histopathologic diagnosis and T1-Weighted Image characteristics in the MRI

Pathologic diagnosis	**T1-Weighting *n (%)***						
	Hypo-		Iso-		Hyper-		TOTAL
Dacryoadenitis	11	(52.4%)	9	(42.9%)	1	(4.8%)	21
Dacryops	4	(100%)	0	(0%)	0	(0%)	4
Pleomorphic adenoma	5	(83.3%)	1	(16.7%)	0	(0%)	6
Adenoid cystic carcinoma	3	(75%)	1	(25%)	0	(0%)	4
Lymphoma	5	(62.5%)	3	(37.5%)	0	(0%)	8
BRLH	1	(33.3%)	1	(33.3%)	1	(33.3%)	3
TOTAL	29 (63%)		15 (32.6%)		2 (4.3%)		46

X^2 = 11.5 (p-value =0.33);
Likelihood Ratio of 10.27 with p-value = 0.417
P-value with Bonferroni correction = 0.00278

Table 31. Crosstabulation of histopathologic diagnosis and T2-Weighted Image characteristics in the MRI

Pathologic diagnosis	**T2-Weighting *n (%)***						
	Hypo-		Iso-		Hyper-		TOTAL
Dacryoadenitis	9	(47.4%)	4	(21.1%)	6	(31.6%)	19
Dacryops	0	(0%)	0	(0%)	3	(100%)	3
Pleomorphic adenoma	2	(28.6%)	1	(14.3%)	4	(57.1%)	7
Adenoid cystic carcinoma	3	(60%)	0	(0%)	2	(40%)	5
Lymphoma	2	(25%)	**5***	**(62.5%)**	1	(12.5%)	8
BRLH	2	(66.7%)	0	(0%)	1	(33.3%)	3
TOTAL	18 (40%)		10 (22.2%)		17 (37.8%)		45

X^2 = 17 (p-value = 0.064);
Likelihood Ratio of 18.09 with p-value = 0.054
*significant p-value of 0.0025
P-value with Bonferroni correction = 0.00278

Table 32. Crosstabulation of histopathologic diagnosis and degree of contrast agent's enhancement in the MRI

Pathologic diagnosis	**Enhancement *n (%)***						
	None		Moderate		High		TOTAL
Dacryoadenitis	2	(7.7%)	13	(50%)	11	(42.3%)	26
Dacryops	**4****	**(80%)**	0	(0%)	1	(20%)	5
Pleomorphic adenoma	0	(0%)	2	(28.6%)	5	(71.4%)	7
Adenoid cystic carcinoma	0	(0%)	4	(80%)	1	(20%)	5
Lymphoma	0	(0%)	9	(90%)	1	(10%)	10
BRLH	0	(0%)	2	(66.7%)	1	(33.3%)	3
Pleomorphic adenocarcinoma	0	(0%)	1	(100%)	0	(0%)	1
TOTAL	6 (10.5%)		31 (54.4%)		20 (35.1%)		57

X^2 = 38.6 (p-value < 0.001);
Cramer's V = 0.58 with p-value < 0.001;
Likelihood Ratio of 30.36 with p-value = 0.001
**significant p-value < 0.0001
P-value with Bonferroni correction = 0.00278

Lastly, dacryops was exclusively hypointense in T1, hyperintense in T2 and exhibited almost no degree of contrast enhancement, with just the occasional peripheral enhancement. This relationship between dacryops and no contrast enhancement was statistically significant (p-value <0.001, p-value with Bonferroni correction = 0.00238), as shown in Table 32.

The logistic regression model based on the clinical data of 63 patients between a correct MRI diagnosis and MRI findings, along with its Hosmer-Lemeshow Test, did not exhibit statistical significance. Its predictive capacity of a correct diagnosis remained at 58.7% from an identical base model value, as can be observed in Table 33. The Nagelkerke R^2 of the model was 5.0%. No variables in the model were statistically significant.

RESULTS

Table 33. Logistic Regression Model: Correct Diagnosis*MRI findings

Base model

Observed CDx[1]	Predicted CDx	
	No	Yes
No	0	26
Yes	0	37

Overall % Correct: 58.7%

Model with Data from clinical signs and symptoms

Observed CDx[1]	Predicted CDx	
	No	Yes
No	0	26
Yes	0	37

Overall % Correct: 58.7%

[1]CDx stands for “correct diagnosis

Model summary

-2 Log likelihood	Cox & Snell R Square	Nagelkerke R Square
83.007	0.037	0.05

p-value = 0.49

Hosmer-Lemeshow Test

Chi-square	df	Significance
0.124	1	0.725

Variables in the model

	B	S.E.	Wald	df	p-value	Exp(B)	BwX
Bone Erosion	0.411	1.254	0.107	1	0.743	1.508	0.001
Margins of lesion	0.179	0.538	0.110	1	0.740	1.196	0.001
Perineural Invasion	20.748	28387	0.000	1	0.999	1.03E+09	0.764

[2]BwX stands for Standardized Beta Weight for X

RESULTS

The course of treatment for the various pathologic diagnoses differed widely, with this being conveyed in Table 34. No enucleations or exenterations were performed. Corticosteroid treatments were not accounted for.

Pleomorphic adenoma and dacryops were wholly excised in 100% of cases. Conversely, dacryoadenitis and BRLH cases were mostly incisionally biopsied (78% of dacryoadenitis cases and 60% of BRLH cases) without performing a complete excision of the lacrimal gland.

Lymphomas were usually biopsied and then referred to our oncology department for adjuvant therapy in the form of radiotherapy, chemotherapy or both (33.3% of patients).

PEMLG treatment varied according to each patient's individual prognosis, with most tumours being fully excised and 7 (64%) patients receiving adjuvant therapy at our oncology department.

Table 34. Treatment according to pathologic diagnosis

	Course of Treatment				
Pathologic diagnosis	A	B	C	D	E
Dacryoadenitis	9/41 (22%)	32/41 (78%)	-	-	-
Lymphoma	4/21 (19%)	10/21 (47.6%)	4/21 (19%)	2/21 (9.5%)	1/21 (4.8%)
Pleomorphic adenoma	13/13 (100%)	-	-	-	-
BRLH	4/10 (40%)	6/10 (60%)	-	-	-
Adenoid cystic carcinoma	-	1/6 (16.7%)	1/6 (16.7%)	4/6 (66.7%)	-
Dacryops	6/6 (100%)	-	-	-	-
Pleomorphic adenocarcinoma	1/5 (20%)	2/5 (40%)	-	1/5 (20%)	1/5 (20%)
Total	37/102 (36.3%)	51/102 (50%)	5/102 (4.9%)	7/102 (6.9%)	2/102 (2%)

A: Excisional Biopsy; B: Incisional Biopsy; C: Biopsy and Radiotherapy; D: Excision and Radiotherapy; E: Excision and Radiotherapy+Chemotherapy

RESULTS

In some patients we did not detect any recurrence of the disease, as portrayed in Table 35. This was the case for patients with pleomorphic adenoma, BRLH, adenoid cystic carcinoma, and dacryops, with an average combined time of follow-up for these four entities of 37.5 ± 57.6 months. The pathologic diagnosis with a higher rate of recurrence was pleomorphic adenocarcinoma: two patients (40%) for an average time of follow-up of 38.6 ± 62.4 months. Lymphoma showed a recurrence rate of 14.3% for an average time of follow-up of 36.7 ± 31.1 months.

Table 35. Recurrence rates and time until recurrence

Pathologic diagnosis	Recurrence	Time of follow-up	Time until Recurrence
Dacryoadenitis	2/45 (4.4%)	23.5 ± 35.5	13 and 107
Lymphoma	3/21 (14.3%)	36.7 ± 31.1	13, 71 and 22
Pleomorphic adenoma	0/13 (0%)	38.9 ± 76	-
BRLH	0/10 (0%)	56.2 ± 62.9	-
Adenoid cystic carcinoma	0/7 (0%)	28.1 ± 20.3	-
Dacryops	0/6 (0%)	14.1 ± 17.4	-
Pleomorphic adenocarcinoma	2/5 (40%)	38.6 ± 62.4	1 and 86

Time unit is Months.

4 - Discussion

The human lacrimal gland can be found in the lacrimal fossa, located supero-laterally to the eye, where it plays a central role in its function (Rouvière & Delmas, 2005).

Indeed, this small tear-shaped gland, hidden from conspicuous examination, is responsible for the adequate refraction of light, nourishment of the cornea, and defense of the ocular surface. It accomplishes all these fundamental tasks through the continuous maintenance of a healthy tear film. In case of impairment, the eye may suffer consequences spanning a wide spectrum of severity, from a mild discomfort in dry eye disease (DED) to complete loss of function in endophthalmitis by a chronic corneal ulcer (Willcox, Argüeso, Georgiev, Holopainen, Laurie, Millar, Papas, Rolland, Schmidt, Stahl, Suarez, Subbaraman, Uçakhan, & Jones, 2017).

From the above, one can comprehend how important it is to recognize and, if required, treat pathology of the human lacrimal gland, especially malignant tumors which can metastasize (Hung, Wei, Huang, Chen, Fuh, & Liao, 2019). As such, this retrospective study endeavored to ascertain the reliability of the current gold-standard diagnostic procedure (MRI) in a clinical setting and to build a model with predictive factors of its reliability, as well as to analyze the collected data with the aim of unlocking meaningful information (Hughes & Miszkiel, 2006; Ueno, Ariji, Izumi, Uetani, Hayashi, & Nakamura, 1996).

4.1 General cohort's clinical data and incidence of human lacrimal gland lesions

Human lacrimal gland lesions are rare and comprehensive prospective population-based studies are lacking in the scientific literature. To date, reporting on the true incidence of tumors of the human lacrimal gland is still pervaded by some degree of error; for example, reports from US databases have varied, as evident when comparing the survey from 645 biopsies of Shields et al. (1984) during a 20-year period and the epidemiological study with 362 patients from 1973 to 2009 of Hassan et al. (2016).

This could be, of course, not only due to the rare nature of these tumors, but also a question of methodology, as alluded to by Shields et al. (1984), with the results being biased by many factors, such as: the specialty of the reviewer; the source of the material; the classification and exclusion criteria used in each study; and the absence of biopsies for some pathological entities like dacryoadenitis (Waleed M. Hassan, Mohamed S. Bakry, Housam M. Hassan, & Ahmad S. Alfaar, 2016; J. A. Shields, Bakewell, Augsburger, & Flanagan, 1984).

Even data such as the proportion between benign and malignant epithelial lesions of the human lacrimal gland carry some uncertainty - in this case, the results were around 60-40 or 50-50, depending on the reports found; these results were summarized by Shields et al. (2004) and are shown below in Table 36 (J. A. Shields, C. L. Shields, J. A. Epstein, R. Scartozzi, & R. C. Eagle, Jr., 2004).

Table 36. Incidence of PEMLG from reports that listed the number of individual tumors (adapted fromJ. A. Shields, C. L. Shields, J. A. Epstein, R. Scartozzi, & R. C. J. Eagle, 2004)

First author	Year	No. PETLG	No. PEMLG	Adenoid cystic carcinoma	Pleomorphic adenocarcinoma	Primary adenocarcinoma	Mucoepidermoid carcinoma	Other not specified
Forrest[7]	1954	26	15	10	1	1		3
Milam and Heath[30]	1956	29	15	14				1
Zimmerman et al[9]	1962	116	38	29	7	2		
Font and Gameb[18]	1978	265	129	79	25	19	4	2
Ni et al[11]	1981	160	70	46	10	4	1	9
Kennedy[37]	1984	17	5	3		2		
Moeloek et al[45]	1987	12	11	9	2			
Shields et al[15]	1989	32	7	2	3		2	
Wright et al[24]	1992	108*	50	38	6	4	1	1
Polito and Leccisotti[31]	1993	36	20	11	7	1	1	
Gunalp and Gunduz[46]	1994	22	8	6	2			
Font et al[20]	1998	41	21	12	7	2		
Johansen et al[47]	2000	52	29	15	6	3	4	1
Shields et al[36]	2003	45	19	14	4		1	
Totals		961*	437* (45%)	288 (66%)‡	80 (18%)‡	38 (9%)‡	14 (3%)‡	17 (4%)‡

As previously alluded to, the main cause of this uncertainty is the small number of patients, as can be seen in the numerous reports listed in Table 36. This same problem was observed in this study. Additionally, however, there are not many ophthalmological orbital surgery specialists in practice in Berlin, and our pool of qualifying patients for this study over a 22-year period topped at 112 patients, despite the Charité Universitätsmedizin Berlin being the state's and nation's biggest hospital (Charité, 2020). This number was further reduced due to the necessary inclusion criteria of our

study, namely the presence of an orbital MRI, a histopathological report of the material and sufficient clinical data.

Since our hospital is the reference hospital for the Berlin region regarding pathologies of the orbit (though not the only one), being in charge of treating the lion's share of patients with lacrimal gland lesions, we tried to attain a rough estimation of the incidence rate for lacrimal gland lesions in the Berlin population (with population data from the Federal Statistical Office of Germany). Due to the small number of cases, we used a multi-year rate to increase the reliability of the result, since enlarging the geographic area was not a viable option (Banerjee & Chaudhury, 2010). The multi-year period which was shown to be more reliable was 2011 to 2018, in light of the following facts: the last population census took place in 2011, meaning that the data sourced was accurate and not a statistical projection; there wasn't population data available for 2019 at the time of writing; and the inclusion rate of patients in our study greatly diminishes before 2010, which can be explained by the deletion of outpatient files from the archive after 10 years, which is where most MRI reports were to be found.

We found that the overall crude incidence rate was 1.93/1,000,000/year [95% CI: 1.67 – 2.2]. This compares well with some other studies, like the one performed in Denmark by von Holstein, where a rate of 1.31/1,000,000/year [95% CI: 1.15-1.49] was calculated, even though our result is surely underestimated, since some lacrimal gland tumors were and continue to be treated in other hospitals in Berlin.

As in von Holstein's comprehensive multi-decade study, we also observed the highest incidence rate in patients between 61 and 70 years old (4.48; 95% CI: 3.24 – 5.73], the lowest incidence rate in patients under 20 years old (0.20; 95% CI: 0 – 0.39] and a positive incidence rate ratio between females and males, meaning that women have a higher risk of being diagnosed with a lacrimal gland tumor. For females, we found this risk to be 1.63 times the risk for males. Again, this compares well to the aforementioned study, which showed an incidence rate ratio of 1.43 (Sarah Linéa von Holstein, Therkildsen, Prause, Stenman, Siersma, & Heegaard, 2013). With a more complete set of data and the inclusion of pre-2011 patients, we could have additionally aimed for a multivariate Poisson regression model to investigate the effects of some variables like age, gender, period of time, district and insurance type on the incidence rate, but we thought that this would go beyond the scope of this current thesis.

Based on these facts, we assumed the viability of our data sample for this study, even though this modest number of cases was by far its greatest limitation. However, as previously shown, this is a categorical problem, instead of a study-specific one.

From the 112 patients included in our study, 73 or ca. 65% were female. Based on more comprehensive studies which show rates of 44% to 60%, we have refrained from assuming any sort of racial predilection, thus ignoring the X^2 value of 10.3 with a p-value <0.001 calculated in Table 8 (Frederick A Jakobiec, 1978; Ni, Kuo, & Dryja, 1992; Seregard & Sahlin, 1999; C. L. Shields, Shields, Eagle, & Rathmell, 1989; Sunderraj, 1991; S. L. von Holstein, Coupland, Briscoe, Le Tourneau, & Heegaard, 2013). The median age of the patients in our study was 55 years, as opposed to the median age of 53 years in the population study from Denmark (1974 to 2007) carried by von Holstein (Sarah Linéa von Holstein, Therkildsen, Prause, Stenman, Siersma, & Heegaard, 2013).

As mentioned previously, tumors of the human lacrimal gland can be grouped as “epithelial” and “non-epithelial”, and further still as benign or malign. This differentiation is of the utmost importance, since each diagnosis leads to a different clinical course and necessary therapy to avoid loss of function or even more serious progression, i.e., a systemic consequence through metastasis.

In this study we found that epithelial lacrimal lesions (*n* = 31) comprised 28.7% of all lacrimal lesions. However, excluding the purely cystic lesions, e.g., dacryops, like some authors chose to, we attained a ratio of 24.5%, which is more in line with the classical 20/80 described in the literature (Johansen, Heegaard, Bogeskov, & Prause, 2000; Kennedy, 1984; J. A. Shields & Shields, 2008). One could speculate that the incidence of non-epithelial lesions is probably understated in our study, since these are less likely to be reported, or can be altogether ignored for patients in some dacryoadenitis cases, which would bring our results closer to this 20/80 ratio. Furthermore, the series and case report literature were based on many patients who were referrals from other hospitals and small practices where an incisional biopsy was first performed in order to disclose the malignant diagnosis, whereas the benign lesions were treated on site. Moreover, most centers in Berlin do not usually perform a biopsy on patients with dacryoadenitis without a trial of systemic steroids or antibiotics

beforehand, so that the number of patients with this non-epithelial lesion is likely to be underreported.

With regards to the epithelial lesions, we achieved a ratio of 52 to 61% for benign lesions, excluding and including dacryops, respectively, which corroborates the usual ratio of ca. 55% seen in the scientific literature and depicted in Table 1 (J. A. Shields, 1989; J. A. Shields, C. L. Shields, J. A. Epstein, R. Scartozzi, & R. C. Eagle, Jr., 2004). Likewise, adenoid cystic carcinoma was shown to be the most common PEMLG (58% of total PEMLG), followed by pleomorphic adenocarcinoma (42%). The proportion of the second deviated somewhat from the 19% presented by Shields et al, while the proportion for the first was identical (J. A. Shields, C. L. Shields, J. A. Epstein, R. Scartozzi, & R. C. Eagle, Jr., 2004).

In terms of non-epithelial lesions, even taking into account the eventual bias of there being less referrals to our hospital of patients with dacryoadenitis due to the reasons explained above, this diagnosis was still the most common of all non-epithelial lesions, with 45 cases totaling 40%. Moreover, lymphoma was identified in 21 cases totaling 19% of all lesions and with almost half (ca. 48%) being of the extranodal marginal zone subtype. The results from both entities compare well with the literature published to date (Ferry, Fung, Zukerberg, Lucarelli, Hasserjian, Preffer, & Harris, 2007; J. A. Shields, C. L. Shields, J. A. Epstein, R. Scartozzi, & R. C. Eagle, Jr., 2004).

4.2 Reliability of magnetic resonance imaging as a diagnostic tool for human lacrimal gland tumors in a clinical setting

It is true that the MRI is the gold standard diagnostic tool, conveying more quality and detail in comparison to CT or US, but its diagnostic reliability for lacrimal gland lesions is unknown (Hesselink & Karampekios, 1996; Hughes & Miszkiel, 2006; Mafee, Edward, Koeller, & Dorodi, 1999). A corollary to this is that, to date, it remains common knowledge that one should examine a human lacrimal gland with recourse to an MRI and that the report presented will be more often correct than not. Nevertheless, the idea for this study was triggered by a degree of unsatisfactory MRI reports in our clinical practice, be it because of unclear/no evident suspected diagnoses, or because of unlikely diagnoses which were later proven incorrect. As an example of these “grey”

reports, we can advance 2 such particular cases from our hospital, one more glaringly erroneous than the other. To wit: the MRI reports submitted for a lymphoma in patient #1 and for a cavernous hemangioma in patient #2. The pathological report revealed a dacryoadenitis and an adenoid cystic carcinoma, respectively.

Bearing such occurrences in mind, we set out to discover to what degree the diagnosis put forward by the radiologist's MRI report on a human lacrimal gland lesion may be relied upon in a clinical setting. To achieve this, we performed a Cohen's kappa test to measure the degree of agreement between the first-line diagnosis of the radiologist and the confirmed pathologic diagnosis. Afterwards, we calculated the accuracy of each individual major MRI diagnosis.

To calculate the degree of agreement from all feasible cases in our clinical practice, we sought the files of all patients where we could properly collect information regarding the suspected diagnosis from the MRI report and the definitive diagnosis from the pathological report. From a total of 107 cases, since five cases had MRI reports which were later deemed to be ambiguous, we then calculated that the degree of correspondence between the pre-operative orbital MRI diagnosis and the histopathologic findings was one of moderate agreement of $k=0.451$ and p-value <0.001, as can be observed in Table 13 (Sun, 2011).

Similar studies can be found in the scientific literature, as in a prospective study by Yildirim et al. (2018), which tried to assess the reliability or predictability of myometrial, lower uterine segment and cervical invasion in endometrial cancer patients through MRI and US, or the study of Tse et al. (2006), which examined the reliability and sensitivity of MRI in the detection and evaluation of the extent of breast tumors, building on comprehensive and numerous previous studies, such as, for example, Kepple et al. (2005) (Kepple, Layeeque, Klimberg, Harms, Siegel, Korourian, Gusmano, & Henry-Tillman, 2005; Tse, Chaiwun, Wong, Yeung, Pang, Tang, & Cheung, 2006; Yildirim, Saatli, Kose, Sancar, Ulukus, Koyuncuoglu, Saygili, & Obuz, 2018).

A study which resembles ours is the one from Luryi et al.. It tried to assess the reliability of the MRI in diagnosing tumors of the cerebellopontine angle, by retrospectivally analysing data from 411 patients from two hospitals in the United States of America. They could find a concordance of 93% between pre-operative MRI-diagnosis and post-operative histological diagnosis. However, this concordance fell to

57.9% when examining tumors other than vestibular schwannoma, which were 91% of the population studied. Furthermore, this study found that the prediction of a MRI diagnosis of vestibular schwannoma was highly sensitive (97%), but less specific (65%), achieving a PPV of 97% and NPV of 76% (Luryi, Michaelides, Babu, Bojrab, Kveton, Hong, Zappia, Sargent, & Schutt, 2019).

Even though many more studies like the abovementioned exist, we could not find such a study for the diagnosis of lacrimal gland lesions with recourse to an MRI.

With regards to the accuracy of the major MRI diagnoses, we could compare our study to Luryi's work. Still, measures of test accuracy are not easily transferable, so this could never be an apples-to-apples comparison (Irwig, Bossuyt, Glasziou, Gatsonis, & Lijmer, 2002). In our study, we could not find a diagnosis with such high measures of sensitivity and PPV, as was the case for vestibular schwannoma in Luryi's study (Luryi, Michaelides, Babu, Bojrab, Kveton, Hong, Zappia, Sargent, & Schutt, 2019). However, all diagnoses had higher rates of specificity, with lymphoma being the lowest at 83%, which carries great relevance in a clinical setting. From all major diagnoses, dacryops stands out with high values for sensitivity and PPV (both at 83%) and even higher for specificity and NPV (99 and 94%). This may be due to two reasons: first, a radiologist only advances the possibility of dacryops if he sees the characteristic peripheral enhancement on application of contrast agent during the MRI examination, a factor which showed a statistically significant relationship to the diagnosis in this study, accompanied by the typical hypointense in T1 and hyperintense in T2 internal composition; second, since it's a well-known pathology, it may be always "top of mind" for the radiologist.

Interestingly, dacryoadenitis, our most common diagnosis, showed low sensitivity (57%) and high specificity (86%), meaning that the radiologists were able to recognize that the pathology involved was not dacryoadenitis in most cases, but on the other hand, they could not accurately recognize a significant number of cases. One could posit this is due to the fact that this entity carries less health risk than the others. In light of this, there may be a bias from the radiologist to not assess somewhat unclear cases as "just" dacryoadenitis and with it, excluding further surgical treatment.

Having calculated the value of overall reliability (k=0.451) of a pre-operative MRI diagnosis and the measures of accuracy for the five major diagnoses, we endeavored

to calculate the same reliability for several groups of patients, with the differentiating factor being a divergent setting employed in the MRI examination. These factors were the strength of magnetic field, the contrast agent, the coils, and multiparametric MR-sequences such as DWI.

From the literature, one learns that an MRI examination of the human lacrimal gland should be performed with a 3 T magnetic field strength, orbital coil and with recourse to multiparametric MR-sequences, since these settings were shown to be significantly better in correctly diagnosing orbital tumors and representing the orbital anatomy. Armed with this knowledge, we, then, grouped the patients accordingly (Erb-Eigner, Warmuth, Taupitz, Bertelmann, Hamm, & Asbach, 2013; Georgouli, Chang, Nelson, James, Tanner, Shelley, Saldana, & McGonagle, 2008; Georgouli, James, Tanner, Shelley, Nelson, Chang, Backhouse, & McGonagle, 2008; Kneeland & Hyde, 1989; Lope, Hutcheson, & Khademian, 2010; Mafee, Rapoport, Karimi, Ansari, & Shah, 2005; Ro, Asbach, Siebert, Bertelmann, Hamm, & Erb-Eigner, 2016; Yuan, Kuai, Chen, & Tao, 2013).

Regarding the magnetic field strength, we could observe that the group of patients which underwent a 3 T MRI examination had a higher reliability (k=0.458) than the group of patients which underwent a 1.5 T examination (k=0.345), as well as higher than the overall result (k=0.451), which corroborates the scientific literature so far. All these results were statistically significant in itself, but not when comparing them to each other.

The results pertaining to the different contrast agents and coils used were disappointing, since they showed an inferior degree of agreement than the overall value, with the result of the group using an orbital coil not being statistically significant. Indeed, we didn't expect to be a material difference in reliability on account of contrast agent used, since there are no reports in the literature indicating an advantage of one over the other in this regard. However, we did expect the group which was examined with recourse to an orbital coil to achieve a better reliability than the overall result, since the literature describes a better signal-to-noise ratio with it, even if its usage comes in detriment of field of examination. Regretablly, this was not the case in our study, with the value observed being k=0.107 and p-value 0.409. Yet, this result was based on only 13 patients and not statistically significant (Erb-Eigner, Warmuth, Taupitz,

Bertelmann, Hamm, & Asbach, 2013; Georgouli, Chang, Nelson, James, Tanner, Shelley, Saldana, & McGonagle, 2008).

Lastly and equally disappointing, the result for the group of patients who underwent DWI sequences showed a poor degree of agreement (k=0.118). This result was also based on a reduced number of patients (nine) and not statistically significant. From the scientific literature, we would have expected the reliability to be higher, which is also our clinical experience (Lope, Hutcheson, & Khademian, 2010; Ro, Asbach, Siebert, Bertelmann, Hamm, & Erb-Eigner, 2016). Here, we can again offer an example, namely a male patient, 70 years-old, who presented at our hospital with a lacrimal gland lesion and an MRI report indicating the presence of an unclear orbital tumor or maybe a pleomorphic adenoma due to undistinguishable margins to the lacrimal gland. A second MRI was then performed, this time at our hospital and with multiparametric sequences. This examination revealed that there was no contact with the lacrimal gland and that it was most likely a cyst, so that surgery could be avoided. In spite of this, the patient preferred the excision of the lesion, so an operation was planned. The pathological report divulged merely the presence of scar tissue, without any evidence of lacrimal gland tissue or malignancy. This exemplifies how the new imaging capabilities may well help us avoid unnecessary surgeries, patient trauma and miscalculated risks, which is why they should be further studied and disseminated more into clinical practice, even though we could not prove such advantages with our work.

It may be comforting to believe in a future flawless reliability of the MRI as a diagnostic tool for lacrimal gland lesions. However, in day-to-day clinical practice, grounded on our calculation in this study of there being “just” a moderate reliability for MRI in the diagnosis of lacrimal gland lesions, with a positive predictive value of around 50% for 3 major entities (pleomorphic adenoma, PEMLG, and lymphoma) and of around 80% for the other 2 (dacryoadenitis and dacryops), it becomes clear that one should not overly rely and base one's clinical thinking solely on the MRI report. Especially when facing the decision of whether to wait and observe or perform surgery, and when deciding the type of surgery (biopsy or direct excision) and how soon it will take place.

DISCUSSION

4.3 Analysis of our cohort's clinical data and search for predictors of a correct image-based diagnosis

4.3.1 Signs and symptoms of human lacrimal gland tumors

The six most common signs and symptoms of a human lacrimal gland lesion are inferior and nasal displacement of the globe, pain, proptosis, swelling of the eyelid, ocular motility restriction and ptosis (AAO, 2016; J. A. Shields, C. L. Shields, J. A. Epstein, R. Scartozzi, & R. C. Eagle, Jr., 2004). Due to the fact that we lacked comprehensive photodocumentation of the clinical presentation of the lacrimal gland lesions, the signs and symptoms on which we based our study had to come directly from the written reports, which in most cases failed to mention the presence of globe dislocation, which is why it was not included in this thesis. Additionally, some data was missing some signs/symptoms in a very small (2) number of patients. On another note, the restriction of ocular motility was interpreted as diplopia, since the two were 100% correlated in the cases analyzed, where information was available. Taking all this into account, we nevertheless posit that the information collected was sufficient enough to draw important conclusions from it.

We found that the chief complaint from 81 (73.6%) patients was swelling of the temporal region of the upper eyelid and the least observed one was pain, with only 9 (8.2%) patients stating it. Since each pathologic diagnosis is known to produce its characteristic signs/symptoms, e.g. with pain being often thought to indicate malignancy, we analyzed the interdependence of the symptoms/signs and the pathological diagnosis with recourse to a Chi-square test (J. A. Shields & Shields, 2008). Here, we were again confronted with the limitations of the small number of cases in this study, the fact that these variables were all categorical, and the fact that our contingency tables' rows and columns couldn't be aggregated in order to run a Fisher's exact test. As such, we had to resort to a Chi-square test with a Monte Carlo estimate for the exact test based on 1 million samples (for which we deliberately chose a confidence level of 99%), since the data violated the Chi-square test assumptions of asymptotic significance (Cohen, 1969). A Bonferroni correction was applied and Cramer's V was used to assess the effect size (Akoglu, 2018). Overall, we were able to observe that there was a statistically significant interdependence between proptosis/swelling and pathologic diagnosis and the Cramer's V value of 0.451 for both

associations corresponded to a very strong association. An ad-hoc analysis showed a statistically significant relationship between: pain and pleomorphic adenocarcinoma (p-value = 0.0025; p-value with Bonferroni correction = 0.00357; see Table 16); proptosis and adenoid cystic carcinoma (p-value = 0.0014; Table 17); swelling and dacryoadenitis (p-value = 0.0034; Table 18); and swelling and BRLH (p-value = 0.0033; Table 18). Such data could help everyday practicing doctors to further guide their clinical suspicion in the diagnosis of a lacrimal gland lesion, attributing, with a higher degree of probability, an otherwise asymptomatic swelling of the eyelid to a dacryoadenitis or BRLH.

Building further from this data set and inspired by some studies where models were created to improve the reliability of the MRI-diagnosis, we set out to build a logistic regression model based on these same five core signs/symptoms, in order to try to find predictors of a correct image-based diagnosis (Swinburne, Schefflein, Sakai, Oermann, Titano, Chen, Tadayon, Aggarwal, Doshi, & Nael, 2019). We found that a model based on these 5 clinical data points for 100 patients had an improved predictive capacity of a correct MRI diagnosis of 64.0%, when comparing to the base model, where only 60.0% of cases were correctly predicted (Table 21). In this model, swelling was shown to be a statistically significant factor (p-value = 0.031) and the Nagelkerke R^2 of the model was 9.0%. However, as a whole, this increased predictive capacity was shown to not be statistically significant, since its p-value was 0.23. Moreover, the Hosmer-Lemeshow Test for our model was not statistically significant (p-value of 0.755), which is a positive outcome, since it means that we could rule out misspecifications in the predictive capacity of our model, had our number of cases been greater. A standardized beta weight for swelling was calculated, coming at 0.116 with an odds ratio of 3.007 [1.108 – 8.160], meaning that for an increase in the logit of 1 of the “swelling” factor, there is a 3 times greater likelihood of the diagnosis being correct, controlling for the other variables (suppressor effect) (Menard, 2011).

Naturally, we could then build a model which just incorporated the variable (swelling), which was shown to be statistically significant, meaning, which was shown to truly have an effect in augmenting the predictive capacity of the model. Done so, we would achieve a Nagelkerke R^2 of 6%, wih a p-value of 0.04. Or even a model with just the 2 variables, which showed the highest standardized beta weight (swelling and pain). This

would achieve a Nagelkerke R^2 of 8%, wih a p-value of 0.05. In spite of that, we consider this to be cherry-picking and not the purpose of this thesis.

Nonetheless, this leaves us wondering if further data inputs or an increased quality of the data could strengthen the predictive capacity of the model, as well as if other predictors could be found in future studies.

4.3.2 Features of the cohort's magnetic resonance imaging data

Encouraged by last section's findings, we repeated the same steps for the collected MRI data. We chose not to include data from CT reports since the number of cases where this was possible was negligible, which reinforced the fact that MRI is the gold-standard diagnostic tool for the human lacrimal gland's pathology (Mafee, Edward, Koeller, & Dorodi, 1999).

The normal lacrimal gland is of moderate, sometimes heterogeneous signal intensity on T1-weighted images and enhances following intravenous contrast agent administration (Hughes & Miszkiel, 2006). As previously reported in Table 5, each lesion of the human lacrimal gland exhibits a particular set of characteristics in MRI, like the adenoid cystic carcinoma being hypo- or isointense in a T1-weighting, iso- or hyperintense in a T2-weighting and presenting a moderate contrast agent enhancement, thus diverging from the normal human lacrimal gland's presentation (Pieper & Thomas, 2014).

Starting with the non-epithelial tumors, we observed that dacryoadenitis did not show constant internal features in T1- and T2-weighting, though contrast enhancement was seldom not observed. On the other hand, lymphomas were mainly hypointense in T1 and isointense in T2, with a moderate degree of contrast enhancement. While examining this data in detail, we encountered a statistically significant relationship between lymphoma and isointense internal features in the T2-weighted image (p-value of 0.0025; p-value with Bonferroni correction = 0.00278; Table 31). With regard to PEMLG, not only the adenoid cystic carcinoma, but also the pleomorphic adenocarcinoma exhibited the expected characteristics, as described in the scientific literature. Lastly, dacryops was exclusively hypointense in T1, hyperintense in T2 and exhibited almost no degree of contrast enhancement, with just the occasional peripheral enhancement. This relation between dacryops and no contrast

enhancement was also statistically significant in the ad-hoc analysis (p-value <0.001, p-value with Bonferroni correction = 0.00238; Table 32) (AAO, 2016; Hughes & Miszkiel, 2006; J. A. Shields, 1989).

Apart from the abovementioned three groups of characteristics, we further analyzed 3 core features of magnetic resonance imaging of the lacrimal gland, as is common practice in scientific literature, these being: bone erosion, configuration of the margins of the lesion and presence of perineural invasion (J. A. Shields & Shields, 2008).

Our study showed a statistically significant interdependence between these 3 core characteristics and pathologic diagnosis, the Cramer V's associations being very strong (0.54 for bone erosion; 0.44 for the margins of the lesion and 0.7 for perineural invasion), as shown in Table 22 (Akoglu, 2018). More specifically, by running an ad-hoc analysis in the same manner as before, we found a statistically significant relationship between: bone erosion and adenoid cystic carcinoma (p-value < 0.001; p-value with Bonferroni correction = 0.00357; see Table 23); and between perineural invasion and pleomorphic adenocarcinoma (p-value < 0.001; Table 24)

On the one hand, one could argue that these results are corroborated by the scientific literature, since bone erosion and perineural invasion are both, indeed, hallmarks of malignant lacrimal lesions, so that our results here are highly relevant (Gunduz, Shields, Gunalp, & Shields, 2003; Ophthalmology, 2016). Nevertheless, on the other hand, we are referring to a cohort of a total of 9 patients in these results, due to which, and despite the known rarity of these pathologies, this loses considerable meaning, and more so in a Chi-square test (Cohen, 1969). The same argument is valid for the two statistically significant relationships found between: lymphoma and isointense internal features in the T2-weighted image; and dacryops and no degree of contrast enhancement.

In addition, one could argue that our collected MRI data was far from optimal, since it also presented the typical limitations of a retrospective imagiological study based on external MRI reports, namely: different machines were used and across a large time period, with all the technological advances/shortfalls this implies; a great number of radiologists were involved in the interpretation of the images with disparate degrees of career and lacrimal gland pathology-specific experience; missing information for some of the data points; different strengths of magnetic field, with a predominant recourse to

1.5 T (75% of a total of 56 reported cases), even though 3 T should be used to improve image quality (Mafee, Rapoport, Karimi, Ansari, & Shah, 2005); different coils, with the head coil being put to use in 65% of all the 37 cases where this was explicitly specified, despite surface-coils being currently recommended for ocular MRI-imaging; different contrast agents utilized, with gadoterate being the most frequent; and diffusion-weighted imaging (DWI) and dynamic contrast enhanced (DCE) sequences were seldom employed (only in 9 patients), which have been shown to further facilitate a correct diagnosis (Erb-Eigner, Warmuth, Taupitz, Bertelmann, Hamm, & Asbach, 2013; Georgouli, Chang, Nelson, James, Tanner, Shelley, Saldana, & McGonagle, 2008; Georgouli, James, Tanner, Shelley, Nelson, Chang, Backhouse, & McGonagle, 2008; Lope, Hutcheson, & Khademian, 2010; Ro, Asbach, Siebert, Bertelmann, Hamm, & Erb-Eigner, 2016; Yuan, Kuai, Chen, & Tao, 2013).

As for the clinical signs/symptoms, a logistic regression model between MRI features and a correct image-based diagnosis was attempted. However, no single feature nor a combination of them was able to increase the predictive capacity of the base model, which may not only be due to its lack of interdependence, but also to the fact that we could only gather sufficient and trustworthy MRI features from the reports of a total of 63 patients, in comparison to clinical data of 100 patients employed in the first model.

4.4 Limitations of this study

Even though we could achieve the primary outcome of this study, that is, assessing the reliability of the MRI as a diagnostic tool, which resulted in a moderate degree of agreement ($k=0.451$, p-value < 0.001, Confidence Interval of 0.34-0.57), our study is not without limitations, the greatest of which being the small number of patients that could be examined, which, of course, diminishes the power of the statistical methods employed. While there were 107 patients with a pre-operative MRI diagnosis and post-operative histopathologic diagnosis, there were only 56 patients with information regarding the strength of magnetic field or even just 9, which underwent an examination with multi-parametric sequences. Unfortunately, due to the rarity of this disease and this having been a monocentric study, there are several examples in our work where a very interesting sub-group analysis, either by filtering through examination differences or by pathologic diagnosis, could not be properly undertaken.

For example, due to the fact of there only being 4 patients with pleomorphic adenocarcinoma, we have to take every statistical analysis performed on this subgroup with a critic mindset. In fact, this was one of the major hurdles to overcome in this study, namely, to decide which statistical method to employ. Firstly, the data was categorical, which complicates an analysis from the start. Second, due to the small number of cases, the Chi-square test assumptions of asymptotic significance were violated, so that we could either use a less reliable Chi-square test with a Monte Carlo estimate for the exact test with a 1% level of significance (in 1 million samples) and Bonferroni correction or somehow structure the data in order to fit a 3x3 table and perform a Fisher's exact test. Since our data could not be grouped without losing most, if not all of its meaning, we had to rely on a Chi-square test with a Monte Carlo estimate. For more trustworthy results, based in methods of asymptotic significance and not in Monte Carlo estimates, most likely a national sourcing of patients would need to be performed.

Another limitation is the quality of the data obtained. Since it is a retrospective study, no standardized criteria were used to define the parameters, which our results depend on. Equally limiting is that our study relies on patients from just one hospital. The results would probably have been more reliable if more patients could have been accepted.

The long span of time for inclusion of patients also originates its own set of limitations, such as: there is a great inter-observer variability, since many ophthalmologists, radiologists, and pathologists were involved; the quality of the MRI examinations increased over the last 20 years, which may have impacted the reliability of the results, although most accepted patients have been treated in the last 10 years, on account of the deletion of outpatient files from the archive after 10 years.

A limitation also arises from the fact that we didn't differentiate between internal and external MRI reports, which could have shown a difference of reliability between the two.

Furthermore, we have no information or way of knowing if the clinical data had an influence in the prediction of the diagnosis by the radiologist or if they only truly relied on the images presented to them.

Lastly, since it is the first study of its kind for this pathology, our results can't be directly compared with the literature, but we welcome further research in this area.

4.5 Other data points and final commentary

Several other data points from the patients' clinical records were collected, but did not offer relevant conclusions, like the best corrected visual acuity and intra-ocular pressure on the first visit and on the first follow-up after surgery; and time from first complaint to first visit. This was due to numerous factors, such as: missing information from the records of some patients (e.g. 44 patients without a value for intra-ocular pressure at the time of the first visit); a low rate of follow-up patients; and questionable reliability of the information, since some patients couldn't pinpoint exactly when the symptoms first began or the records were vague in this regard, and since the measurements of BCVA and IOP were not only undertaken by different individuals, but also by different methods for the IOP, i.e., mostly Goldmann applanation tonometry (GAT) or non-contact tonometry (NCT), with some studies showing statistically significant differences (G. Demirci, Erdur, Tanriverdi, Gulkilik, & Ozsutcu, 2019).

All in all, our secondary outcomes have to be taken with a grain of salt due to the subpar quality of the data, as well as due to the reduced number of cases and categorical variables, which therefore invalidates high-power statistical studies or highly meaningful and far-reaching conclusions. Nevertheless, the entire exercise enabled us to find some interesting associations and promising predictive models, which may well serve to focus future research in this direction.

Finally, we could observe that there is a moderate reliability of the MRI diagnosis in human lacrimal gland tumors, with the positive predictive value being highest for dacryops and dacryoadenitis. This reliability was even higher for MRI examinations carried out with a 3 T magnetic strength field. Furthermore, some interesting and relevant associations between signs and symptoms and diagnosis, as well as MRI characteristics and diagnosis could be found. Swelling was shown to be the only variable capable of increasing the predictive capacity of a logistic regression model.

5 - References

AAO. (2016). *Basic and Clinical Science Course* (Vol. Fundamentals and Principles of Ophthalmology): American Academy of Ophthalmology.

Akoglu, H. (2018). User's guide to correlation coefficients. *Turkish Journal of Emergency Medicine, 18*. doi:10.1016/j.tjem.2018.08.001

Azzarolo, A. M., Mircheff, A. K., Kaswan, R. L., Stanczyk, F. Z., Gentschein, E., Becker, L., Nassir, B., & Warren, D. W. (1997). Androgen support of lacrimal gland function. *Endocrine, 6*(1), 39-45. doi:10.1007/BF02738800

Banerjee, A., & Chaudhury, S. (2010). Statistics without tears: Populations and samples. *Industrial psychiatry journal, 19*(1), 60-65. doi:10.4103/0972-6748.77642

Bartley, G. B., & Harris, G. J. (2002). Adenoid cystic carcinoma of the lacrimal gland: is there a cure...yet? *Ophthalmic Plast Reconstr Surg, 18*(5), 315-318. doi:10.1097/00002341-200209000-00001

Botelho, S. Y., Hisada, M., & Fuenmayor, N. (1966). Functional innervation of the lacrimal gland in the cat. Origin of secretomotor fibers in the lacrimal nerve. *Arch Ophthalmol, 76*(4), 581-588. doi:10.1001/archopht.1966.03850010583019

Charité. (2020). Zahlen und Fakten. Retrieved from https://www.charite.de/die_charite/profil/zahlen_fakten/

Chen, Q., Wang, J., Tao, A., Shen, M., Jiao, S., & Lu, F. (2010). Ultrahigh-resolution measurement by optical coherence tomography of dynamic tear film changes on contact lenses. *Investigative ophthalmology & visual science, 51*(4), 1988-1993. doi:10.1167/iovs.09-4389

Cockerham, G. C., & Jakobiec, F. A. (1997). Lymphoproliferative disorders of the ocular adnexa. *Int Ophthalmol Clin, 37*(4), 39-59. doi:10.1097/00004397-199703740-00005

Cohen, J. (1969). *Statistical Power Analysis for the Behavioral Sciences*: Academic Press.

Dartt, D. A. (2002). Regulation of mucin and fluid secretion by conjunctival epithelial cells. *Prog Retin Eye Res, 21*(6), 555-576. doi:10.1016/s1350-9462(02)00038-1

de la Cuadra-Blanco, C., Peces-Peña, M. D., & Mérida-Velasco, J. R. (2003). Morphogenesis of the human lacrimal gland. *Journal of anatomy, 203*(5), 531-536. doi:10.1046/j.1469-7580.2003.00233.x

Dean, C., Ito, M., Makarenkova, H. P., Faber, S. C., & Lang, R. A. (2004). Bmp7 regulates branching morphogenesis of the lacrimal gland by promoting mesenchymal proliferation and condensation. *Development (Cambridge, England), 131*(17), 4155-4165. doi:10.1242/dev.01285

del Castillo, J. M. (1981). *Dacriología básica: ponencia oficial de la Sociedad Española de Oftalmología, Las Palmas, 1981*: Universidad de La Laguna, Departamento de Oftalmología.

Demirci, G., Erdur, S. K., Tanriverdi, C., Gulkilik, G., & Ozsutcu, M. (2019). Comparison of rebound tonometry and non-contact airpuff tonometry to Goldmann applanation tonometry. *Ther Adv Ophthalmol, 11*, 2515841419835731. doi:10.1177/2515841419835731

Demirci, H., Shields, C. L., Shields, J. A., Honavar, S. G., Mercado, G. J., & Tovilla, J. C. (2002). Orbital tumors in the older adult population. *Ophthalmology, 109*(2), 243-248. doi:https://doi.org/10.1016/S0161-6420(01)00932-0

Duke-Elder, S. (1961). Wybar K. System of Ophthalmology. Vol. II: The Anatomy of the Visual System. *St. Louis*.

Duke-Elder, S. (1970). System of Ophthalmology V. *Ophthalmic Optics & Refraction*.

Duke, T. G., Fahy, G. T., & Brown, L. J. (2000). Adenoid cystic carcinoma of the superonasal conjunctival fornix. *Orbit, 19*(1), 31-35.

An epidemiological survey of lacrimal fossa lesions in Japan: number of patients and their sex ratio by pathological diagnosis. (2005). *Jpn J Ophthalmol, 49*(5), 343-348. doi:10.1007/s10384-005-0224-x

Erb-Eigner, K., Warmuth, C., Taupitz, M., Bertelmann, E., Hamm, B., & Asbach, P. (2013). Ocular MR imaging: evaluation of different coil setups in a phantom study. *Magn Reson Med Sci, 12*(3), 177-182. doi:10.2463/mrms.2012-0081

Eter, N., & Gobbels, M. (2002). A new technique for tear film fluorophotometry. *Br J Ophthalmol, 86*(6), 616-619. doi:10.1136/bjo.86.6.616

Farmer, D. J. T., Nathan, S., Finley, J. K., Shengyang Yu, K., Emmerson, E., Byrnes, L. E., Sneddon, J. B., McManus, M. T., Tward, A. D., & Knox, S. M. (2017). Defining epithelial cell dynamics and lineage relationships in the developing lacrimal gland. *Development (Cambridge, England), 144*(13), 2517-2528. doi:10.1242/dev.150789

Farmer, J. P., Lamba, M., Lamba, W. R., Jordan, D. R., Gilberg, S., Sengar, D. P. S., Bence-Bruckler, I., & Burns, B. F. (2005). Lymphoproliferative lesions of the lacrimal gland: clinicopathological, immunohistochemical and molecular genetic analysis. *Canadian Journal of Ophthalmology, 40*(2), 151-160. doi:https://doi.org/10.1016/S0008-4182(05)80026-2

Ferry, J. A., Fung, C. Y., Zukerberg, L., Lucarelli, M. J., Hasserjian, R. P., Preffer, F. I., & Harris, N. L. (2007). Lymphoma of the ocular adnexa: A study of 353 cases. *Am J Surg Pathol, 31*(2), 170-184. doi:10.1097/01.pas.0000213350.49767.46

Font, R. L., Smith, S. L., & Bryan, R. G. (1998). Malignant Epithelial Tumors of the Lacrimal Gland: A Clinicopathologic Study of 21 Cases. *Archives of Ophthalmology, 116*(5), 613-616. doi:10.1001/archopht.116.5.613

Foster, W. J., Jr, Kraus, M. D., & Custer, P. L. (2003). Herpes Simplex Virus Dacryoadenitis in an Immunocompromised Patient. *Archives of Ophthalmology, 121*(6), 911-913. doi:10.1001/archopht.121.6.911

Foulks, G. N., & Bron, A. J. (2003). Meibomian gland dysfunction: a clinical scheme for description, diagnosis, classification, and grading. *Ocul Surf, 1*(3), 107-126. doi:10.1016/s1542-0124(12)70139-8

Frome, E. L. (1983). The Analysis of Rates Using Poisson Regression Models. *Biometrics, 39*(3), 665-674. doi:10.2307/2531094

Fullard, R. J., & Snyder, C. (1990). Protein levels in nonstimulated and stimulated tears of normal human subjects. *Investigative ophthalmology & visual science, 31*(6), 1119-1126.

Fullard, R. J., & Tucker, D. (1994). Tear protein composition and the effects of stimulus. *Adv Exp Med Biol, 350*, 309-314. doi:10.1007/978-1-4615-2417-5_52

Fullard, R. J., & Tucker, D. L. (1991). Changes in human tear protein levels with progressively increasing stimulus. *Investigative ophthalmology & visual science, 32*(8), 2290-2301.

Georgouli, T., Chang, B., Nelson, M., James, T., Tanner, S., Shelley, D., Saldana, M., & McGonagle, D. (2008). Use of high-resolution microscopy coil MRI for depicting orbital anatomy. *Orbit, 27*(2), 107-114. doi:10.1080/01676830701558166

Georgouli, T., James, T., Tanner, S., Shelley, D., Nelson, M., Chang, B., Backhouse, O., & McGonagle, D. (2008). High-resolution microscopy coil MR-Eye. *Eye (Lond), 22*(8), 994-996. doi:10.1038/sj.eye.6702755

Gipson, I. K., & Argueso, P. (2003). Role of mucins in the function of the corneal and conjunctival epithelia. *Int Rev Cytol, 231*, 1-49. doi:10.1016/s0074-7696(03)31001-0

Gordon, L. K. (2006). Orbital inflammatory disease: a diagnostic and therapeutic challenge. *Eye (Lond), 20*(10), 1196-1206. doi:10.1038/sj.eye.6702383

Govindarajan, B., & Gipson, I. K. (2010). Membrane-tethered mucins have multiple functions on the ocular surface. *Exp Eye Res, 90*(6), 655-663. doi:10.1016/j.exer.2010.02.014

Gunduz, K., Shields, C. L., Gunalp, I., & Shields, J. A. (2003). Magnetic resonance imaging of unilateral lacrimal gland lesions. *Graefes Arch Clin Exp Ophthalmol, 241*(11), 907-913. doi:10.1007/s00417-003-0748-z

Hassan, W. M., Bakry, M. S., Hassan, H. M., & Alfaar, A. S. (2016). Incidence of orbital, conjunctival and lacrimal gland malignant tumors in USA from Surveillance, Epidemiology and End Results, 1973-2009. *International journal of ophthalmology, 9*(12), 1808-1813. doi:10.18240/ijo.2016.12.18

Hassan, W. M., Bakry, M. S., Hassan, H. M., & Alfaar, A. S. (2016). Incidence of orbital, conjunctival and lacrimal gland malignant tumors in USA from Surveillance, Epidemiology and End Results, 1973-2009. *Int J Ophthalmol, 9*(12), 1808-1813. doi:10.18240/ijo.2016.12.18

Henderson, J. W., & Farrow, G. M. (1980). Primary malignant mixed tumors of the lacrimal gland. Report of 10 cases. *Ophthalmology, 87*(6), 466-475. doi:10.1016/s0161-6420(80)35206-8

Hesselink, J. R., & Karampekios, S. (1996). Normal computed tomography and magnetic resonance imaging anatomy of the globe, orbit, and visual pathways. *Neuroimaging Clin N Am, 6*(1), 15-27.

Higgins, R. A., Blankenship, J. E., & Kinney, M. C. (2008). Application of immunohistochemistry in the diagnosis of non-Hodgkin and Hodgkin lymphoma. *Arch Pathol Lab Med, 132*(3), 441-461. doi:10.1043/1543-2165(2008)132[441:Aoiitd]2.0.Co;2

Holly, F. J., & Lemp, M. A. (1977). Tear physiology and dry eyes. *Survey of Ophthalmology, 22*(2), 69-87. doi:https://doi.org/10.1016/0039-6257(77)90087-X

Hornblass, A., Friedman, A. H., & Yagoda, A. (1981). Erosion of the orbital plate (frontal bone) by a benign tumor of the lacrimal gland. *Ophthalmic Surg, 12*(10), 737-743.

Hughes, G. K., & Miszkiel, K. A. (2006). Imaging of the lacrimal gland. *Semin Ultrasound CT MR, 27*(6), 476-491. doi:10.1053/j.sult.2006.09.002

Hung, J. Y., Wei, Y. H., Huang, C. H., Chen, L. W., Fuh, C. S., & Liao, S. L. (2019). Survival outcomes of eye-sparing surgery for adenoid cystic carcinoma of lacrimal gland. *Jpn J Ophthalmol, 63*(4), 344-351. doi:10.1007/s10384-019-00671-w

Irwig, L., Bossuyt, P., Glasziou, P., Gatsonis, C., & Lijmer, J. (2002). Designing studies to ensure that estimates of test accuracy are transferable. *BMJ (Clinical research ed.), 324*(7338), 669-671. doi:10.1136/bmj.324.7338.669

Jakobiec, F. A. (1978). *Ocular and adnexal tumors* (Vol. 2): Aesculapius Publishing Company.

Jakobiec, F. A. (1982). *Ocular anatomy, embryology, and teratology*: Harpercollins.

Jakobiec, F. A., Yeo, J. H., Trokel, S. L., Abbott, G. F., Anderson, R., Citrin, C. M., & Alper, M. G. (1982). Combined Clinical and Computed Tomographic Diagnosis of Primary Lacrimal Fossa Lesions. *American Journal of Ophthalmology, 94*(6), 785-807. doi:https://doi.org/10.1016/0002-9394(82)90304-X

Johansen, S., Heegaard, S., Bogeskov, L., & Prause, J. U. (2000). Orbital space-occupying lesions in Denmark 1974-1997. *Acta Ophthalmol Scand, 78*(5), 547-552. doi:10.1034/j.1600-0420.2000.078005547.x

Karatza, E. C., Shields, C. L., Shields, J. A., & Eagle, R. C., Jr. (2004). Calcified orbital cyst simulating a malignant lacrimal gland tumor in an adult. *Ophthalmic Plast Reconstr Surg, 20*(5), 397-399. doi:10.1097/01.iop.0000139527.83345.64

Kennedy, R. E. (1984). An evaluation of 820 orbital cases. *Transactions of the American Ophthalmological Society, 82*, 134.

Kepple, J., Layeeque, R., Klimberg, V. S., Harms, S., Siegel, E., Korourian, S., Gusmano, F., & Henry-Tillman, R. S. (2005). Correlation of magnetic resonance imaging and pathologic size of infiltrating lobular carcinoma of the breast. *The American journal of surgery, 190*(4), 623-627.

Kim, S. H., Hwang, S., Kweon, S., Kim, T. K., & Oh, J. (2005). Two cases of lacrimal gland agenesis in the same family--clinicoradiologic findings and management. *Can J Ophthalmol, 40*(4), 502-505. doi:10.1016/s0008-4182(05)80014-6

King-Smith, E., Fink, B., Hill, R., Koelling, K., & Tiffany, J. (2004). The thickness of the tear film. *Current Eye Research, 29*(4-5), 357-368. doi:10.1080/02713680490516099

King, J. E. (2007). Standardized Coefficients in Logistic Regression. *Paper presented at the annual meeting of the Southwest Educational Research Association. Baylor College of Medicine. San Antonio.*

Kneeland, J. B., & Hyde, J. S. (1989). High-resolution MR imaging with local coils. *Radiology, 171*(1), 1-7. doi:10.1148/radiology.171.1.2648466

Knowles, D. M., Jakobiec, F. A., McNally, L., & Burke, J. S. (1990). Lymphoid hyperplasia and malignant lymphoma occurring in the ocular adnexa (orbit, conjunctiva, and eyelids): a prospective multiparametric analysis of 108 cases during 1977 to 1987. *Hum Pathol, 21*(9), 959-973. doi:10.1016/0046-8177(90)90181-4

Krawczuk-Hermanowiczowa, O. (1983). [Effect of sex hormones on the lacrimal gland. Effect of testosterone, estradiol and both hormones together on the morphological appearance of the lacrimal gland in the castrated rat]. *Klin Oczna, 85*(10), 337-339. Retrieved from https://www.ncbi.nlm.nih.gov/pubmed/6664034

Kuppens, E. V., Stolwijk, T. R., de Keizer, R. J., & van Best, J. A. (1992). Basal tear turnover and topical timolol in glaucoma patients and healthy controls by fluorophotometry. *Investigative ophthalmology & visual science, 33*(12), 3442-3448.

Lemke, A.-J., Hosten, N., Foerster, P. I., & Felix, R. (2001). Schnittbilddiagnostik von OrbitatumorenTeil 2: Extrakonales Kompartiment, subperiostales Kompartiment, Tränendrüse, Bulbus, präseptales Kompartiment. *Der Radiologe, 41*(6), 520-529. doi:10.1007/s001170051067

Lieb, W. E. (1998). Color Doppler imaging of the eye and orbit. *Radiol Clin North Am, 36*(6), 1059-1071. doi:10.1016/s0033-8389(05)70231-1

Liesegang, T. J. (1993). Ocular adnexal lymphoproliferative lesions. *Mayo Clin Proc, 68*(10), 1003-1010. doi:10.1016/s0025-6196(12)62275-7

Lope, L. A., Hutcheson, K. A., & Khademian, Z. P. (2010). Magnetic resonance imaging in the analysis of pediatric orbital tumors: Utility of diffusion-weighted imaging. *Journal of*

American Association for Pediatric Ophthalmology and Strabismus, 14(3), 257-262. doi:https://doi.org/10.1016/j.jaapos.2010.01.014

Lorber, M., & Vidic, B. (2009). Measurements of lacrimal glands from cadavers, with descriptions of typical glands and three gross variants. *Orbit, 28*(2-3), 137-146. doi:10.1080/01676830902766014

Lorenzano, D., & Rose, G. E. (2017). The "Wedge Sign": An Imaging Sign for Aggressive Lacrimal Gland Disease. *Ophthalmology, 124*(7), 1081-1083. doi:https://doi.org/10.1016/j.ophtha.2017.03.004

Luryi, A. L., Michaelides, E. M., Babu, S., Bojrab, D. I., Kveton, J. F., Hong, R. S., Zappia, J., Sargent, E. W., & Schutt, C. A. (2019). Reliability of clinical diagnosis of masses of the cerebellopontine angle: A retrospective multi-institutional study. *American Journal of Otolaryngology, 40*(2), 133-136. doi:https://doi.org/10.1016/j.amjoto.2019.01.009

Mafee, M. F., Edward, D. P., Koeller, K. K., & Dorodi, S. (1999). Lacrimal gland tumors and simulating lesions. Clinicopathologic and MR imaging features. *Radiol Clin North Am, 37*(1), 219-239, xii. doi:10.1016/s0033-8389(05)70089-0

Mafee, M. F., Rapoport, M., Karimi, A., Ansari, S. A., & Shah, J. (2005). Orbital and ocular imaging using 3- and 1.5-T MR imaging systems. *Neuroimaging Clin N Am, 15*(1), 1-21. doi:10.1016/j.nic.2005.02.010

Mausolf, F. A. (1975). *The Anatomy of the Ocular Adnexa: Guide to Orbital Dissection*: Charles C. Thomas Publisher.

Menard, S. (2011). Standards for Standardized Logistic Regression Coefficients. *Social Forces, 89*(4), 1409-1428. doi:10.1093/sf/89.4.1409

Mishima, S., Gasset, A., Klyce, S. D., Jr., & Baum, J. L. (1966). Determination of tear volume and tear flow. *Invest Ophthalmol, 5*(3), 264-276.

Moore, K. L., & Persaud, T. V. N. (2008). *The Developing Human* (8th ed.): Elsevier.

Morandi, F., Valerio, E., & Cutrone, M. (2016). Congenital lacrimal fistula. *Arch Dis Child Fetal Neonatal Ed, 101*(1), F66. doi:10.1136/archdischild-2015-309044

Nagendran, S., Alsamnan, M., Strianese, D., & Malhotra, R. (2020). Ectopic Lacrimal Gland Tissue: A Systematic Review. *Ophthalmic Plast Reconstr Surg*. doi:10.1097/iop.0000000000001621

Netter, F. H. (2018). *Atlas of Human Anatomy* (7th ed.): Elsevier.

Ni, C., Kuo, P. K., & Dryja, T. P. (1992). Histopathological classification of 272 primary epithelial tumors of the lacrimal gland. *Chin Med J (Engl), 105*(6), 481-485.

Nichols, K. K., Foulks, G. N., Bron, A. J., Glasgow, B. J., Dogru, M., Tsubota, K., Lemp, M. A., & Sullivan, D. A. (2011). The international workshop on meibomian gland dysfunction: executive summary. *Investigative ophthalmology & visual science, 52*(4), 1922-1929. doi:10.1167/iovs.10-6997a

Obata, H., Yamagami, S., Saito, S., Sakai, O., & Tsuru, T. (2003). A case of acute dacryoadenitis associated with herpes zoster ophthalmicus. *Jpn J Ophthalmol, 47*(1), 107-109. doi:10.1016/s0021-5155(02)00645-7

Olsen, T. G., & Heegaard, S. (2019). Orbital lymphoma. *Surv Ophthalmol, 64*(1), 45-66. doi:10.1016/j.survophthal.2018.08.002

Ophthalmology, A. A. o. (2016). *Basic and Clinical Science Course* (Vol. Orbit, Eyelids, and Lacrimal System).

Paulino, A. F. G., & Huvos, A. G. (1999). Epithelial tumors of the lacrimal glands: A clinicopathologic study. *Annals of Diagnostic Pathology, 3*(4), 199-204. doi:https://doi.org/10.1016/S1092-9134(99)80051-3

Paulsen, F. P., Schaudig, U., & Thale, A. B. (2003). Drainage of tears: impact on the ocular surface and lacrimal system. *Ocul Surf, 1*(4), 180-191. doi:10.1016/s1542-0124(12)70013-7

Peng, C.-C., Cerretani, C., Li, Y., Bowers, S., Shahsavarani, S., Lin, M., & Radke, C. (2014). Flow evaporimeter to assess evaporative resistance of human tear-film lipid layer. *Industrial & Engineering Chemistry Research, 53*(47), 18130-18139.

Pieper, C. C., & Thomas, D. (2014). Bildgebung der Tränendrüse und der Tränenwege. [Imaging of the lacrimal gland and the lacrimal drainage system]. *Radiologie up2date, 14*(04), 307-328. doi:10.1055/s-0034-1390790

Razek, A. A., Elkhamary, S., & Mousa, A. (2011). Differentiation between benign and malignant orbital tumors at 3-T diffusion MR-imaging. *Neuroradiology, 53*(7), 517-522. doi:10.1007/s00234-011-0838-2

Reese, A. B. (1956). The Treatment of Expanding Lesions of the Orbit *: With Particular Regard to Those Arising in the Lacrimal Gland the Seventh Arthur J. Bedell Lecture. *American Journal of Ophthalmology, 41*(1), 3-11. doi:10.1016/0002-9394(56)91457-X

Rhem, M. N., Wilhelmus, K. R., & Jones, D. B. (2000). Epstein-Barr virus dacryoadenitis. *American Journal of Ophthalmology, 129*(3), 372-375. doi:https://doi.org/10.1016/S0002-9394(99)00351-7

Ro, S.-R., Asbach, P., Siebert, E., Bertelmann, E., Hamm, B., & Erb-Eigner, K. (2016). Characterization of orbital masses by multiparametric MRI. *European Journal of Radiology, 85*(2), 324-336. doi:10.1016/j.ejrad.2015.11.041

Rose, G. E., & Wright, J. E. (1992). Pleomorphic adenoma of the lacrimal gland. *The British journal of ophthalmology, 76*(7), 395-400. doi:10.1136/bjo.76.7.395

Rouvière, H., & Delmas, A. (2005). *Anatomie humaine: Descriptive, topographique et fonctionnelle* (XI ed. Vol. Tête et cou): Elsevier.

Ruskell, G. L. (2004). Distribution of pterygopalatine ganglion efferents to the lacrimal gland in man. *Exp Eye Res, 78*(3), 329-335. doi:10.1016/j.exer.2003.06.001

Rusu, M. C. (2010). Microanatomy of the neural scaffold of the pterygopalatine fossa in humans: trigeminovascular projections and trigeminal-autonomic plexuses. *Folia Morphol (Warsz), 69*(2), 84-91.

Scott, G., Balsiger, H., Kluckman, M., Fan, J., & Gest, T. (2014). Patterns of innervation of the lacrimal gland with clinical application. *Clin Anat, 27*(8), 1174-1177. doi:10.1002/ca.22447

Seregard, S., & Sahlin, S. (1999). Panorama of orbital space-occupying lesions. The 24-year experience of a referral centre. *Acta Ophthalmologica Scandinavica, 77*(1), 91-98.

Sherman, D. D., Gonnering, R. S., Wallow, I. H., Lemke, B. N., Doos, W. G., Dortzbach, R. K., Lyon, D. B., & Bindley, C. D. (1993). Identification of orbital lymphatics: enzyme histochemical light microscopic and electron microscopic studies. *Ophthalmic Plast Reconstr Surg, 9*(3), 153-169.

Sheskin, D. J. (2004). *Handbook of Parametric and Nonparametric statistical procedures* (C. H. C.-W. C. S. University Ed. 3rd ed.).

Shields, C. L., Shields, J. A., Eagle, R. C., & Rathmell, J. P. (1989). Clinicopathologic review of 142 cases of lacrimal gland lesions. *Ophthalmology, 96*(4), 431-435.

Shields, J. A. (1989). *Epithelial tumors of the lacrimal gland - Diagnosis and Management of Orbital Tumors* (W. S. Co Ed.).

Shields, J. A., Bakewell, B., Augsburger, J. J., & Flanagan, J. C. (1984). Classification and Incidence of Space-Occupying Lesions of the Orbit: A Survey of 645 Biopsies. *Archives of Ophthalmology, 102*(11), 1606-1611. doi:10.1001/archopht.1984.01040031296011

Shields, J. A., & Shields, C. L. (1987). Malignant transformation of presumed pleomorphic adenoma of lacrimal gland after 60 years. *Arch Ophthalmol, 105*(10), 1403-1405. doi:10.1001/archopht.1987.01060100105037

Shields, J. A., & Shields, C. L. (2008). *Eyelid, conjunctival, and orbital tumors : atlas and textbook* (2 ed.): Lippincott Williams & Wilkins.

Shields, J. A., Shields, C. L., Eagle, R. C., Jr., Adkins, J., & De Potter, P. (1997). Adenoid cystic carcinoma developing in the nasal orbit. *Am J Ophthalmol, 123*(3), 398-399. doi:10.1016/s0002-9394(14)70138-2

Shields, J. A., Shields, C. L., Epstein, J. A., Scartozzi, R., & Eagle, R. C., Jr. (2004). Review: primary epithelial malignancies of the lacrimal gland: the 2003 Ramon L. Font lecture. *Ophthalmic Plast Reconstr Surg, 20*(1), 10-21. doi:10.1097/01.Iop.0000103003.87842.Bb

Shields, J. A., Shields, C. L., Epstein, J. A., Scartozzi, R., & Eagle, R. C. J. (2004). Primary Epithelial Malignancies of the Lacrimal Gland: The 2003 Ramon L. Font Lecture. *Ophthalmic Plastic & Reconstructive Surgery, 20*(1), 10-21. doi:10.1097/01.Iop.0000103003.87842.Bb

Shields, J. A., Shields, C. L., & Scartozzi, R. (2004). Survey of 1264 patients with orbital tumors and simulating lesions: The 2002 Montgomery Lecture, part 1. *Ophthalmology, 111*(5), 997-1008. doi:https://doi.org/10.1016/j.ophtha.2003.01.002

Sibony, P. A., Walcott, B., McKeon, C., & Jakobiec, F. A. (1988). Vasoactive intestinal polypeptide and the innervation of the human lacrimal gland. *Arch Ophthalmol, 106*(8), 1085-1088. doi:10.1001/archopht.1988.01060140241033

Šimundić, A.-M. (2009). Measures of Diagnostic Accuracy: Basic Definitions. *EJIFCC, 19*(4), 203-211. Retrieved from https://pubmed.ncbi.nlm.nih.gov/27683318

https://www.ncbi.nlm.nih.gov/pmc/articles/PMC4975285/

Smith, S., & Rootman, J. (1986). Lacrimal ductal cysts. Presentation and management. *Surv Ophthalmol, 30*(4), 245-250. doi:10.1016/0039-6257(86)90120-7

Stein, H. A. S., Raymond M.; Freeman, Melvin I. (2012). *The Ophthalmic Assistant: A Text for Allied and Associated Ophthalmic Personnel: Expert Consult - Online and Print* (9th ed.): Elsevier.

Stevenson, W., Pugazhendhi, S., & Wang, M. (2016). Is the main lacrimal gland indispensable? Contributions of the corneal and conjunctival epithelia. *Surv Ophthalmol, 61*(5), 616-627. doi:10.1016/j.survophthal.2016.02.006

Stewart, W. B., Krohel, G. B., & Wright, J. E. (1979). Lacrimal gland and fossa lesions: an approach to diagnosis and management. *Ophthalmology, 86*(5), 886-895. doi:10.1016/s0161-6420(79)35467-7

Sullivan, D. A., Edwards, J. A., Wickham, L. A., Pena, J. D. O., Gao, J., Ono, M., & Kelleher, R. S. (1996). Identification and endocrine control of sex steroid binding sites in the lacrimal gland. *Current Eye Research, 15*(3), 279-291. doi:10.3109/02713689609007622

Sun, S. (2011). Meta-analysis of Cohen's kappa. *Health Services and Outcomes Research Methodology, 11*(3), 145-163. doi:10.1007/s10742-011-0077-3

Sunderraj, P. (1991). Malignant tumours of the eye and adnexa. *Indian J Ophthalmol, 39*(1), 6-8.

Swerdlow, S. H., Campo, E., Pileri, S. A., Harris, N. L., Stein, H., Siebert, R., Advani, R., Ghielmini, M., Salles, G. A., & Zelenetz, A. D. (2016). The 2016 revision of the World Health Organization classification of lymphoid neoplasms. *Blood, 127*(20), 2375-2390.

Swinburne, N. C., Schefflein, J., Sakai, Y., Oermann, E. K., Titano, J. J., Chen, I., Tadayon, S., Aggarwal, A., Doshi, A., & Nael, K. (2019). Machine learning for semi-automated classification of glioblastoma, brain metastasis and central nervous system lymphoma using magnetic resonance advanced imaging. *Ann Transl Med, 7*(11), 232. doi:10.21037/atm.2018.08.05

Tan, K. O., Sack, R. A., Holden, B. A., & Swarbrick, H. A. (1993). Temporal sequence of changes in tear film composition during sleep. *Curr Eye Res, 12*(11), 1001-1007. doi:10.3109/02713689309029226

Tellado, M. V., McLean, I. W., Specht, C. S., & Varga, J. (1997). Adenoid cystic carcinomas of the lacrimal gland in childhood and adolescence. *Ophthalmology, 104*(10), 1622-1625. doi:10.1016/s0161-6420(97)30086-4

Tse, G. M. K., Chaiwun, B., Wong, K.-T., Yeung, D. K., Pang, A. L. M., Tang, A. P. Y., & Cheung, H. S. (2006). Magnetic resonance imaging of breast lesions—a pathologic correlation. *Breast Cancer Research and Treatment, 103*(1), 1. doi:10.1007/s10549-006-9352-3

Ueno, H., Ariji, E., Izumi, M., Uetani, M., Hayashi, K., & Nakamura, T. (1996). MR imaging of the lacrimal gland. Age-related and gender-dependent changes in size and structure. *Acta Radiol, 37*(5), 714-719. doi:10.1177/02841851960373p259

Vaidhyanath, R., Kirke, R., Brown, L., & Sampath, R. (2008). Lacrimal Fossa Lesions: Pictorial Review of CT and MRI Features. *Orbit, 27*(6), 410-418. doi:10.1080/01676830802333667

von Holstein, S. L., Coupland, S. E., Briscoe, D., Le Tourneau, C., & Heegaard, S. (2013). Epithelial tumours of the lacrimal gland: a clinical, histopathological, surgical and oncological survey. *Acta Ophthalmol, 91*(3), 195-206. doi:10.1111/j.1755-3768.2012.02402.x

von Holstein, S. L., Therkildsen, M. H., Prause, J. U., Stenman, G., Siersma, V. D., & Heegaard, S. (2013). Lacrimal gland lesions in Denmark between 1974 and 2007. *Acta Ophthalmologica, 91*(4), 349-354. doi:10.1111/j.1755-3768.2012.02403.x

Waller, R. R., Riley, F. C., & Henderson, J. W. (1973). Malignant mixed tumor of the lacrimal gland. Occult source of metastatic carcinoma. *Arch Ophthalmol, 90*(4), 297-299. doi:10.1001/archopht.1973.01000050299010

Weber, A. L., Romo, L. V., & Sabates, N. R. (1999). PSEUDOTUMOR OF THE ORBIT: Clinical, Pathologic, and Radiologic Evaluation. *Radiologic Clinics of North America, 37*(1), 151-168. doi:https://doi.org/10.1016/S0033-8389(05)70084-1

Weis, E., Rootman, J., Joly, T. J., Berean, K. W., Al-Katan, H. M., Pasternak, S., Bonavolontà, G., Strianese, D., Saeed, P., Feldman, K. A., Vangveeravong, S., Lapointe, J. S., & White, V. A. (2009). Epithelial Lacrimal Gland Tumors: Pathologic Classification and Current Understanding. *Archives of Ophthalmology, 127*(8), 1016-1028. doi:10.1001/archophthalmol.2009.209

Werb, A. (1983). The anatomy of the lacrimal system. *The lacrimal system*, 23-32.

White, V. A. (2019). Understanding and Classification of Ocular Lymphomas. *Ocul Oncol Pathol, 5*(6), 379-386. doi:10.1159/000499845

Willcox, M. D. P., Argüeso, P., Georgiev, G. A., Holopainen, J. M., Laurie, G. W., Millar, T. J., Papas, E. B., Rolland, J. P., Schmidt, T. A., Stahl, U., Suarez, T., Subbaraman, L. N., Uçakhan, O. Ö., & Jones, L. (2017). TFOS DEWS II Tear Film Report. *The ocular surface, 15*(3), 366-403. doi:10.1016/j.jtos.2017.03.006

Witmer, M. (2009). Unraveling the Difficult Diagnosis of Dacryoadenitis. Retrieved from https://www.reviewofophthalmology.com/article/unraveling-the-difficult-diagnosis-of-dacryoadenitis

Wolff, E. (1946). The muco-cutaneous junction of the lidmargin and the distribution of the tear fluid. *Trans Ophthalmol Soc UK, 66*, 291-308.

Wright, J. E., Stewart, W. B., & Krohel, G. B. (1979). Clinical presentation and management of lacrimal gland tumours. *Br J Ophthalmol, 63*(9), 600-606. doi:10.1136/bjo.63.9.600

Xu, Y., Cheung, Y. B., Lam, K. F., Tan, S. H., & Milligan, P. (2010). A simple approach to the estimation of incidence rate difference. *American journal of epidemiology, 172*(3), 334-343. doi:10.1093/aje/kwq099

Yildirim, N., Saatli, B., Kose, S., Sancar, C., Ulukus, C., Koyuncuoglu, M., Saygili, U., & Obuz, F. (2018). Predictability of myometrial, lower uterine segment and cervical invasion with 3D transvaginal ultrasonography and magnetic resonance imaging in endometrial cancer patients: a prospective cohort study. *Med Ultrason, 20*(3), 348-354. doi:10.11152/mu-1493

Yuan, Y., Kuai, X. P., Chen, X. S., & Tao, X. F. (2013). Assessment of dynamic contrast-enhanced magnetic resonance imaging in the differentiation of malignant from benign orbital masses. *Eur J Radiol, 82*(9), 1506-1511. doi:10.1016/j.ejrad.2013.03.001

Zhang, F., Sha, Y., Qian, J., Huang, W.-h., Li, X.-F., Wang, S.-j., & Ye, X.-P. (2014). Role of magnetic resonance diffusion-weighted imaging in differentiating lacrimal masses. *Journal of Magnetic Resonance Imaging, 40*(3), 641-648. doi:10.1002/jmri.24392

6 - Eidesstattliche Versicherung

„Ich, Sergio Filipe Alves Macedo, versichere an Eides statt durch meine eigenhändige Unterschrift, dass ich die vorgelegte Dissertation mit dem Thema: „Zuverlässigkeit der MRT bei der Diagnose eines Tränendrüsentumors und Anzeichen einer korrekten bildgebenden Diagnose“ / „Reliability of the magnetic resonance imaging as a diagnostic tool for lacrimal gland tumors and predictors of a correct image-based diagnosis“ selbstständig und ohne nicht offengelegte Hilfe Dritter verfasst und keine anderen als die angegebenen Quellen und Hilfsmittel genutzt habe.

Alle Stellen, die wörtlich oder dem Sinne nach auf Publikationen oder Vorträgen anderer Autoren/innen beruhen, sind als solche in korrekter Zitierung kenntlich gemacht. Die Abschnitte zu Methodik (insbesondere praktische Arbeiten, Laborbestimmungen, statistische Aufarbeitung) und Resultaten (insbesondere Abbildungen, Graphiken und Tabellen) werden von mir verantwortet.

Meine Anteile an etwaigen Publikationen zu dieser Dissertation entsprechen denen, die in der untenstehenden gemeinsamen Erklärung mit dem Erstbetreuer, angegeben sind. Für sämtliche im Rahmen der Dissertation entstandenen Publikationen wurden die Richtlinien des ICMJE (International Committee of Medical Journal Editors; www.icmje.og) zur Autorenschaft eingehalten. Ich erkläre ferner, dass ich mich zur Einhaltung der Satzung der Charité – Universitätsmedizin Berlin zur Sicherung Guter Wissenschaftlicher Praxis verpflichte.

Weiterhin versichere ich, dass ich diese Dissertation weder in gleicher noch in ähnlicher Form bereits an einer anderen Fakultät eingereicht habe.

Die Bedeutung dieser eidesstattlichen Versicherung und die strafrechtlichen Folgen einer unwahren eidesstattlichen Versicherung (§§156, 161 des Strafgesetzbuches) sind mir bekannt und bewusst.“

Datum Unterschrift

_____

Unterschrift, Datum und Stempel Prof. Dr. med. Eckart Bertelmann

_____

Unterschrift des Doktoranden

7 – Lebenslauf

Mein Lebenslauf wird aus datenschutzrechtlichen Gründen in der elektronischen Version meiner Arbeit nicht veröffentlicht.

Mein Lebenslauf wird aus datenschutzrechtlichen Gründen in der elektronischen Version meiner Arbeit nicht veröffentlicht.

8 – Publikationsliste

1. Macedo S, Pohlmann D, Lenglinger M, Pleyer U, Joussen AM, Winterhalter S. Optical coherence tomography angiography (OCTA) findings in Serpiginous Choroiditis. *BMC Ophthalmol*. 2020;20(1):258. Published 2020 Jun 30. doi:10.1186/s12886-020-01527-5
2. Pohlmann D, Macedo S, Stübiger N, Pleyer U, Joussen AM, Winterhalter S. Multimodal Imaging in Birdshot Retinochoroiditis. *Ocul Immunol Inflamm*. 2017;25(5):621-632. doi:10.1080/09273948.2017.1375532
3. Pohlmann D, Barth A, Macedo S, Pleyer U, Winterhalter S, Albayrak Ö. The impact of impending / onset of vision loss on depression, anxiety, and vision-related quality of life in Birdshot-Retinochoroiditis and Serpiginous Choroiditis. *PLoS One.* 2020 Oct 5;15(10):e0239210. doi: 10.1371/journal.pone.0239210.

9 – Danksagung

An dieser Stelle möchte ich mich bei allen bedanken, die mir zum Schreiben einer Dissertation/Promotionsarbeit angeraten haben. Es war ein sehr lehrreiches Erlebnis und eine Zeit mit vielen Höhen und Tiefen.

Zuerst gebührt mein Dank Herrn Prof. Eckart Bertelmann, der mich immer motiviert hat und meine Promotionsarbeit unermüdlich betreut hat. Von ihm konnte ich immer hilfreiche Kommentare und konstruktive Kritik erwarten und dafür möchte ich mich herzlich bedanken.

Ein besonderer Dank gilt allen Mitarbeitern und Kollegen der Augenklinik, für die konstante Unterstützung und freundschaftliche Zusammenarbeit.

Außerdem möchte ich mich bei Frau Gunawardana vom Institut für Biometrie und Klinische Epidemiologie für die kompetente Beratung bedanken.

Abschließend möchte ich mich bei meiner Familie und Freundin bedanken, die stets ein offenes Ohr für mich hatten und schlicht aus dem Grund, dass sie Menschen sind, auf die ich immer zählen kann.